Disponible en www.hormigonyacero.com
Hormigón y Acero 2023; 74(299-300):169-186
https://doi.org/10.33586/hya.2023.3124

Design of Steel Fibre Reinforced Concrete Structures According to the Annex L of the Eurocode-2 2023

Diseño de estructuras de hormigón reforzado con fibras de acero según el Anejo L del nuevo Eurocódigo-2 2023

de la Fuente, A.[a], Monserrat-López, A.[*,b], Tošić, N.[a], Serna, P.[c]

[a] *Department of Civil and Environmental Engineering, UPC-BarcelonaTECH.*
[b] *Department of Civil and Environmental Engineering, UPC-BarcelonaTECH; Postdoctoral Margarita Salas Fellowship funded by UPV.*
[c] *Institute of Concrete Science and Technology ICITECH Universitat Politècnica de València.*

Recibido el 20 de febrero de 2023; aceptado el 30 de marzo de 2023

ABSTRACT

The Annex L of FprEN 1992-1-1:2023 (EC-2) provides provisions for the design of Steel Fibre Reinforced Concrete (SFRC) structures. This Annex is supported by a comprehensive background document (BD) that gathers the main outcomes of the research carried out on SFRC during the last thirty years. This paper aims to cover the sections of Annex L and supplement those with scientific literature, to help readers reach a deeper understating of the fundamentals and specific details of the proposed formulations and rules.

KEYWORDS: Fibre reinforced concrete, design, standardization, Eurocode 2, steel fibre.

RESUMEN

El Anexo L del FprEN 1992-1-1:2023 (EC-2) plantea disposiciones para el diseño de estructuras de hormigón reforzado con fibras de acero (SFRC). Este anexo está respaldado por un sólido documento de antecedentes (BD) que recopila los principales resultados de las investigaciones realizadas sobre SFRC durante los últimos treinta años. Este artículo tiene como objetivo cubrir las secciones del Anexo L y complementarlas con literatura científica para permitir que los lectores profundicen en los fundamentos y detalles específicos de las formulaciones y reglas establecidas.

PALABRAS CLAVE: Hormigón reforzado con fibras, diseño, estandarización, Eurocódigo 2, fibras de acero.

1. INTRODUCTION

Provisions for the structural design of Steel Fibre Reinforced Concrete (SFRC) members were included in both FprEN 1992-1-1:2023 (Annex L) [1] and FprEN 1992-1-2:2023 (Annex B) [2]. This has been the result of increasing demand for regulations of this materials from the construction sector; well-stablished knowledge on the mechanical properties of SFRC derived from the research and wide variety of successful existing applications (Figure 1) and the future perspectives for the material [3].

In this regard, chronologically at European level, the DBV 2001 [4] was the first to introduce design provisions for SFRC structures in Germany, followed by the RILEM TC 162-TDF in 2003 [5], the Italian CNR-DT/204/2006 in Italy [6] and the EHE-08 in Spain [7]. Within these 20 years, other European countries have regulated the design of SFRC structures. Even, in some national regulations (i.e., Italy, Spain and Sweden [6–8]), the use of other types of fibre materials (mainly synthetic-based) for partially replacing the ordinary steel reinforcement are regulated by including specifications related to the mechanical properties of these materials. In the same line, the fib Model Code 2010 [40], also covers the use of SFRC (and other types of FRCs).

Furthermore, the type of reinforcement for concrete has

* Persona de contacto / *Corresponding author*:
Correo-e / *e-mail*: andrea.monserrat@upc.edu (Andrea Monserrat-López).

How to cite this article: De la Fuente, A., Moserrat-López, A., Tošić, N., & Serna, P. (2023) Design of Steel Fibre Reinforced Concrete Structures According to the Annex L of the Eurocode-2 2023, Hormigón y Acero 74(299-300):169-186, https://doi.org/10.33586/hya.2023.3124

proved to have a significant impact on the sustainability performance of the structure. Some researchers were focused on quantifying the sustainability performance -considering economic, environmental and social indicators- of concrete structures reinforced with different types and configuration of reinforcements (including traditional RC, SFRC, and hybrid solutions) [9–11]. The outcomes of these analyses prove—and confirm—that the sustainability performance of SFRC and hybrid reinforced (steel fibres + steel rebar) concrete solutions are promising.

This paper is aimed to cover—not exhaustively—the features included in the Annexes L and B of the FprEN 1992-1-1:2023 [1] and FprEN 1992-1-2:2023 [2], respectively (both referred to as EC-2 hereafter), and complement those with justifications and explanations supported by the Background Document (BD) to Annex L [12] and scientific literature, when necessary.

2. DESIGN BASIS - SAFETY FORMAT

The design approach for SFRC structures proposed in the EC-2 is aligned with the partial safety format described in Eurocode 0 [13]. In this regard, the material partial safety factor (γ_{sf}) for SFRC to be considered for both compression and tensile mechanical properties is established as 1.50 for both persistent and transient situation in ULS, 1.20 for accidental situations and 1.00 for SLS. These safety factors are equivalent to those suggested in the EC-2 for reinforced and/or prestressed concrete structures.

As acknowledged in the BD and other relevant literature dealing with the design basis FRC [12,14], the post-cracking (residual hereinafter) tensile properties of this material are known to be subjected to several sources of uncertainty. Fibre distribution and orientation anisotropy are the dominant sources of variability that lead to a total scatter in the notched beam test EN 14651 [15] ranging between 10% to 30% [16,17] depending on the amount of fibres, fresh concrete properties, and other aspects [18]. This scatter observed in the EN 14651 beams tends to be superior to that observed in the final structure due to the usually larger volume of SFRC involved in the cracked areas of the latter. The combined use of: characteristic values of the residual flexural tensile strength ($f_{R,k}$); orientation factors (k_o) [19–21] and the factor k_G for taking into account the decrease of variability with the increase of the size of cracked areas (with respect to the EN 14651 beam, 125 × 150 mm²), allows for designs that meet the structural reliability levels widely accepted for traditional reinforced concrete (RC) structures [22].

In specific structures or components, different partial safety factors might be required for optimization purposes or to meet other failure consequences classes (with other reliability levels associated). To this end, FORM [23] has been already implemented to calibrate γ_{sf} for precast FRC tunnel linings [24] and for FRC elements without transversal reinforcement [25]. Alternatively, and specifically oriented to non-linear structural analysis, the method proposed in [26] to calibrate the global resistance safety factor -and reported in the Annex F of the EC-2- was satisfactorily used and implemented in SFRC flat slabs [27–29]. The test up to failure of the SFRC flat slab (200 mm thickness, and four bays of 5 × 6 m) presented in [29] (see Figure 2) proved that the design carried out combining FE-based non-linear models and the safety factor calibration approach [26] lead to safe-side results for the ultimate load [30].

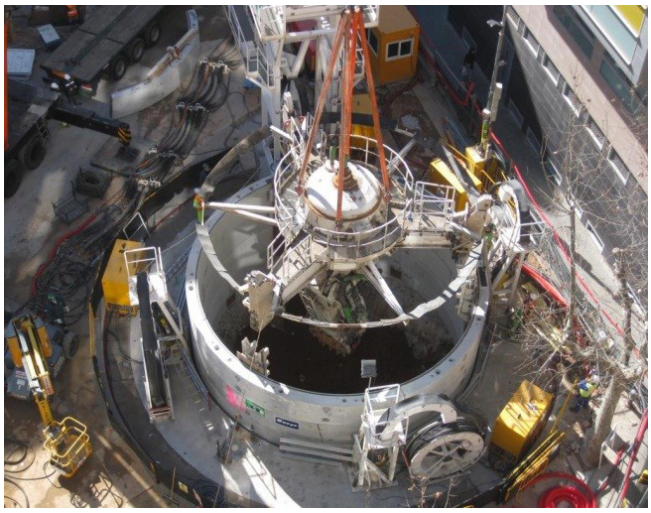

(a)

(b)

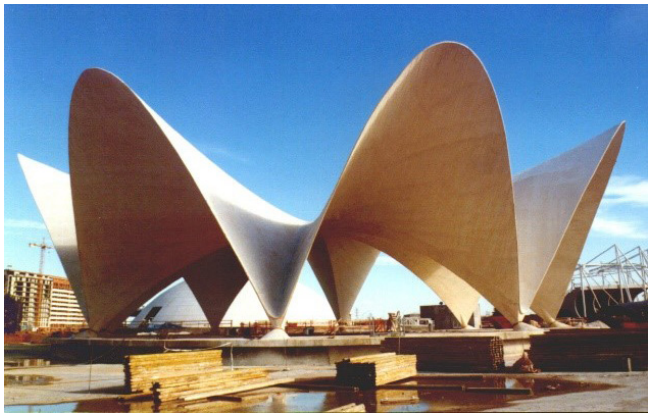

(c)

Figure 1. Different existing applications of SFRC in (a) underground construction (tunnel vertical shaft in Barcelona, Spain), (b) building column-supported flat slab (LKS Headquarters Building in Mondragón, Spain) and (c) architectural applications (Culvert of the Oceanographic Restaurant in Valencia, Spain).

(a)

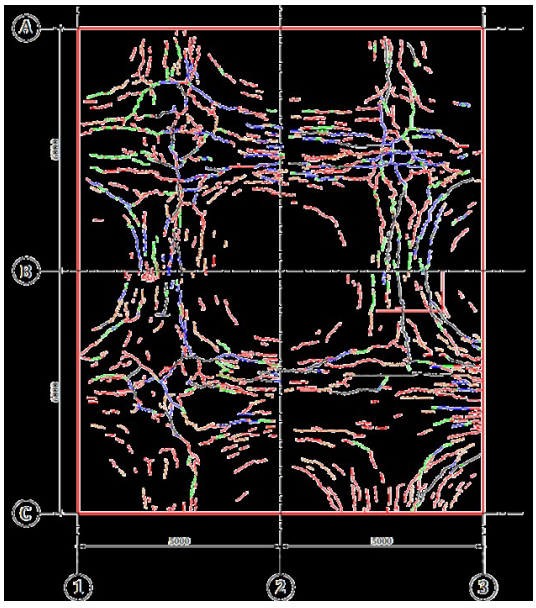

(b)

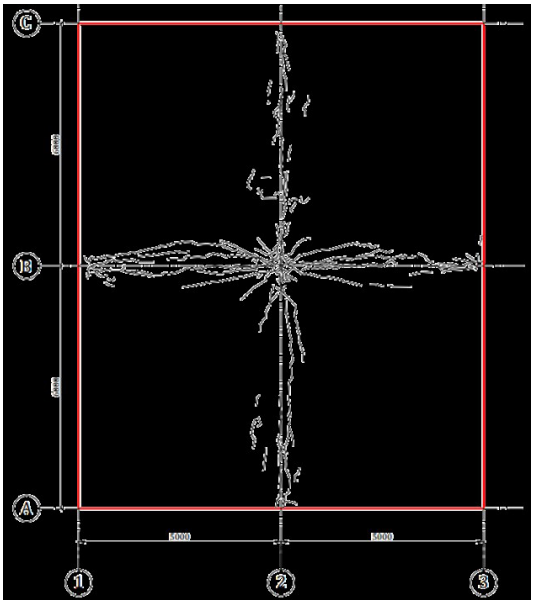

(c)

Figure 2. Real-scale test of the SFRC flat slab reported in [29]: (a) application of the live load, and final crack patterns of the (b) bottom and (c) upper sides of the slab.

3. MATERIALS

3.1. General aspects

The EC-2 explicitly refers to steel fibres (SF) that follow the requirements of the EN 14889-1 [31] as concrete reinforcement with the capacity to replace or complement the ordinary steel reinforcement. SFs are seen as a material that enhances the residual capacity of the resulting SFRC composite for both compression (confinement effect) and tension (cracking control, ductility and energy absorption capacity).

The adequate selection of both fibre geometry and strength for a specific mix design can lead to an efficient application. The best solution requires a compromise among the targeted effect of the fibres in different limit states. In this regard, and in general terms, short and thin fibres might be suitable for initial crack control while these not affect significantly the workability of the composite. On the opposite, long and slender –with performant anchorages– fibres might be suitable when higher residual tensile strength of the SFRC is required for crack control in SLS and bearing capacity in ULS. In this case, the impact on workability may be significant. These tendencies are more evident for high fibres' dosages, and the mechanical effects tend to be empowered with the matrix quality [32]. The workability reduction has to be compensated using plasticizer admixtures, and, for high fibres dosages, the mix design has to be adapted with finer granulometries.

3.2. Strength and ductility classification

In general, the addition of fibres does not modify matrix properties as density, both compressive and tensile (pre-cracked) strengths, elastic modulus, and shrinkage for the range of strength classes (SC) identified in the Annex L (Table l.2).

Concerning creep, both compressive and tensile (pre-cracking) creep of SFRC can be computed according to 5.1 of the EC-2. However, if tensile-creep is expected to be a design determining parameter in any limit state, tests must be conducted following a standardized testing configuration and procedure [33–35] to quantify its time-dependent magnitude (see Figure 3). According to [36], tensile-creep of SFRC may be significant in elements with both low degree of redundancy and low amounts of longitudinal reinforcement.

Assuming these starting points, EC-2 typifies the SFRC SC based on the residual flexural strength (f_R) of the composite determined according to EN 14651 [15] (see Figure 4). The characteristic values of the residual flexural strengths for crack mouth opening displacements (CMODs) of 0.5 mm and 2.5 mm, $f_{R,1k}$ and $f_{R,3k}$, are the relevant design, strength characterization and quality control parameters of the SFRC [37]. This statistical values of fR account for the sources of variability of samples of the same and of different batches. $f_{R,1k}$ and $f_{R,3k}$ shall be computed considering that: f_R follows a log-normal probability density distribution according to EN 1990 [13] (5% quantile, 75% of confidence level); and that the standard deviation of fR is unknown unless explicitly agreed. Criteria to determine the statistic properties of f_R and to assess the population standard deviation could be found in [38,39].

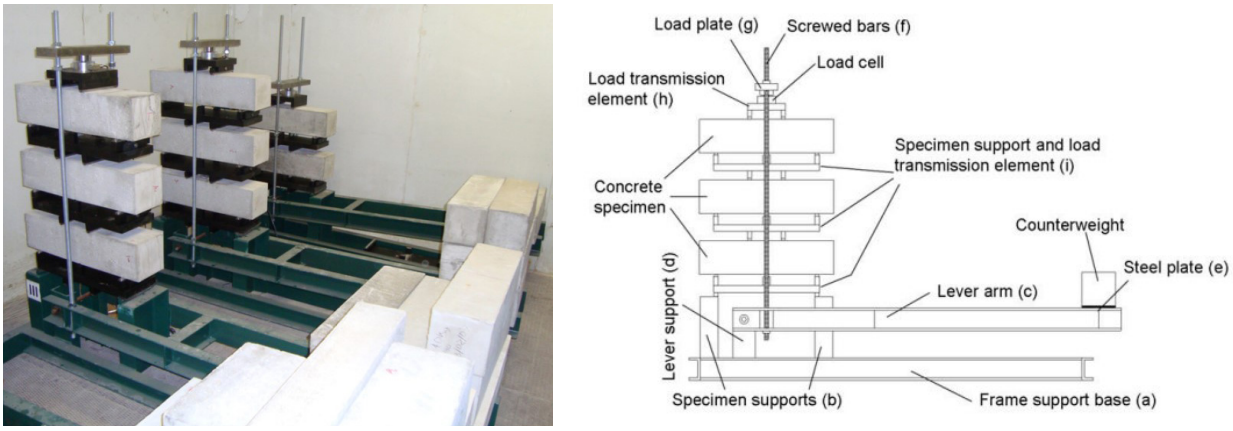

Figure 3. Test configuration for quantifying creep time-dependant phenomena in pre-cracked FRC beams subjected to long-term flexure [33–35].

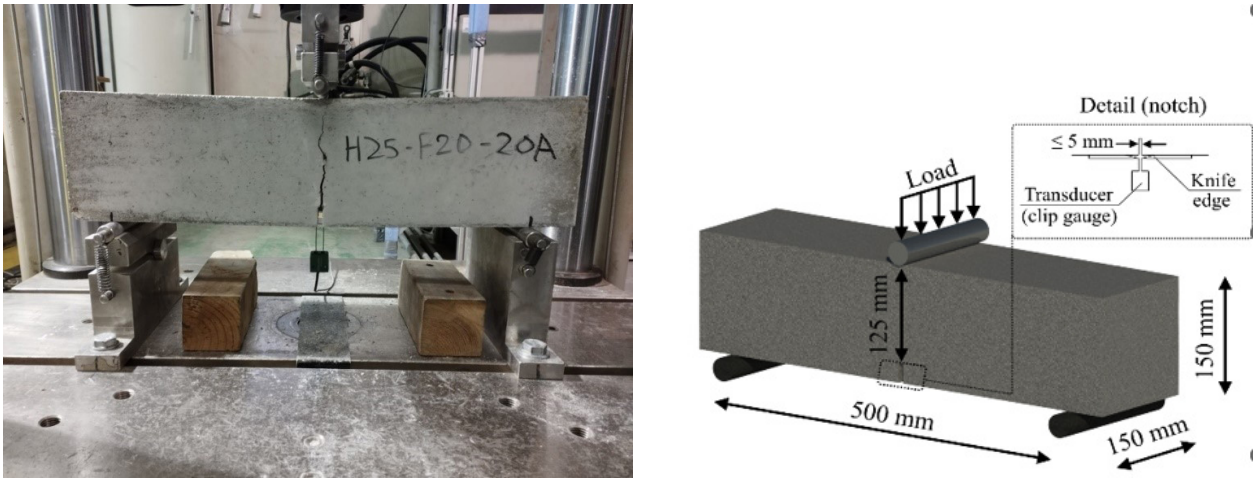

Figure 4. Test setup according to EN 14651 [15].

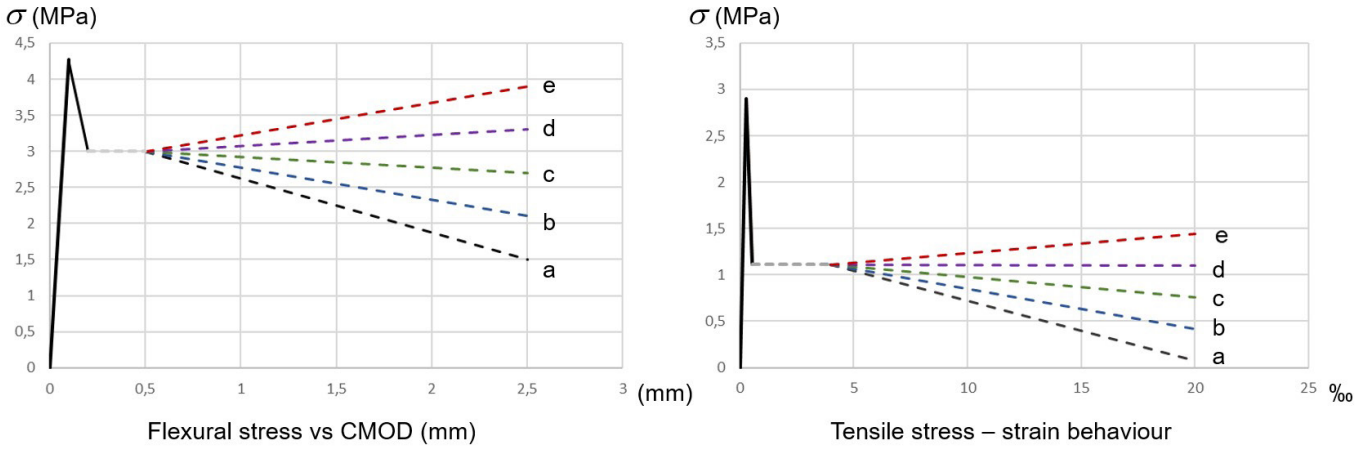

Figure 5. Limits for the ductility classes in the EN 14651 [15]: (a) flexural test for a FRC corresponding to a SC 3, and (b) the resultant tensile stress/strain law evaluated according to EC-2.

The value of $f_{R,1k}$ establish the strength class: SC (1.0; 1.5; 2.0; 2.5; 3.0; 3.5; 4.0; 4.5; 5.0; 6.0; 7.0; 8.0) and the ductility class is denominated by a letter "a", "b", "c", "d" or "e" when the ratio $f_{R,3k}$ /SC exceeds the values of 0.5; 0.7; 0.9; 1.1 or 1.3 respectively. Figure 5 represents an example for those limits by means of a qualitative tensile stress-CMOD relationship.

This SFRC classification criteria is non-coincident with the initial proposal in the MC2010 [40], where the ductility class is defined, with the same limits, but based on the $f_{R,3k}$ / $f_{R,1k}$ ratio instead of the $f_{R,3k}$/SC ratio. In this sense, the EC-2 criterion is oriented to accept the compensation of a low ductility by an increase in strength. For instance, a concrete SC4

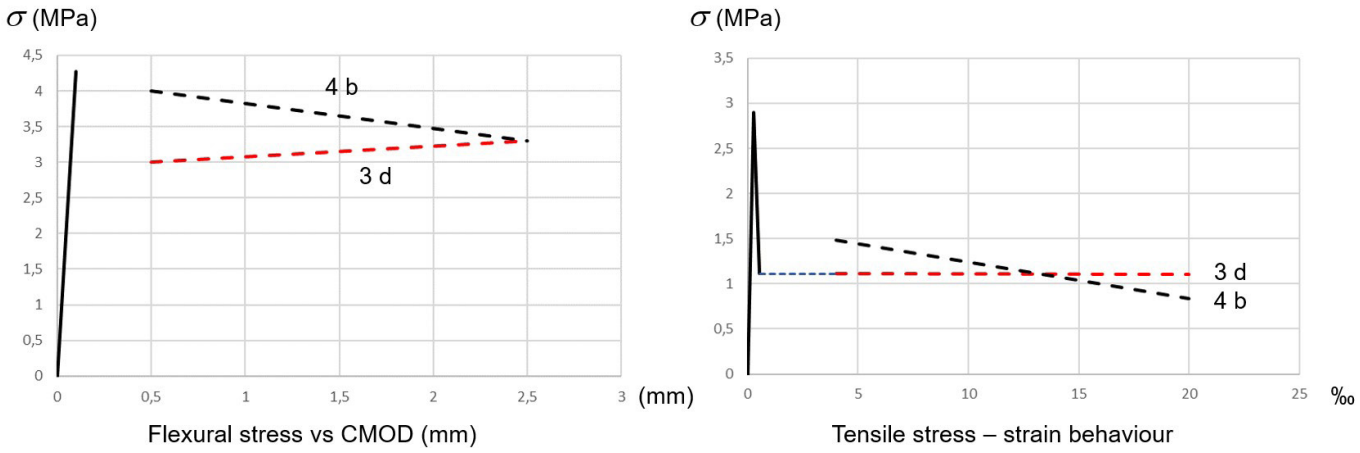

Figure 6. Example of accepted FRC concretes when a SC3d class is prescribed.

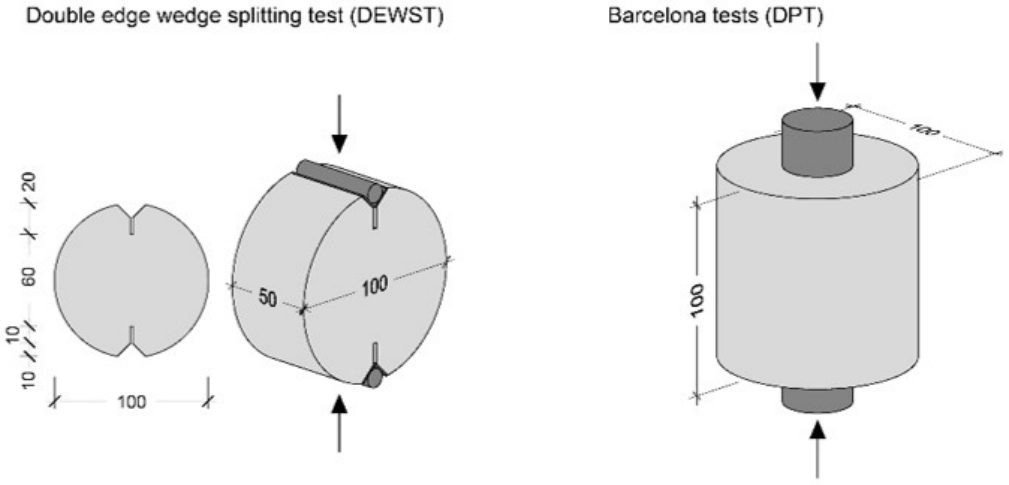

Figure 7. Dimensions and boundary conditions for the DEWST and DPT.

b could be accepted as a SC3 d as shown in Figure 6.

Even if the EC-2 does not make any explicit mention, only for quality control (QC) purposes, alternative tests as the DEWS [41] and the Double Punching Test (DPT, or BCN test) [42–44] (see Figure 7) may be used provided an statistically coherent and robust correlation [45] with the notched beam EN-14651 [15] has been established for the SFRC under characterization.

3.3. *Design assumptions for the material*

As per cross-sectional analysis and design, the design values of the service and ultimate residual strength of SLS (f_{Ftsd}) and ULS (f_{Ftud}), respectively, should be computed with Eq. 1 and 2, respectively.

$$f_{Ftsd} = f_{Fts,ef}/\gamma_{SF} = k_o\, k_G\, 0.37\, f_{R,1k}/\gamma_{SF} \quad (1)$$

$$f_{Ftud} = f_{Ftu,ef}/\gamma_{SF} = k_o\, k_G\, 0.33\, f_{R,3k}/\gamma_{SF} \quad (2)$$

where k_o is the factor that relates the fibre orientation expected in the real structure with that existing in the notched beam EN-14651 [15] and k_G is the factor accounting for the effect of member size.

The Annex L suggests considering k_o = 0.5 unless otherwise is specified in the same Annex L or verified by testing, with final values always smaller than 1.7. Likewise, for bending, shear and torsion forces k_o = 1.0 may be used when S2-S4 consistency classes (according to EN 206 [46]) are achieved.

The orientation factor can be assessed by means of representative tests [20]: cutting and testing beams from the real structure and/or using non-destructive tests based on the inductive properties of the SFRC [47–50]. Concerning the latter, the SFRC flat slab constructed and tested up to failure reported in [29] was cored for characterizing the amount, distribution and orientation of fibres with a portable inductive device (see Figure 8). The orientation factor pattern was posteriorly computed by means of the results obtained. An equivalent approach was conducted in SFRC slabs [46] with conclusive results towards the alternative use of these non-destructive techniques.

The size effect on the magnitude of variation coefficient of the SFRC residual tensile properties is considered through the coefficient k_G (=1.0 + 0.5 A_{ct} ≤ 1.5), which depends on the area of the tension zone (A_{ct}) involved in the flexural failure mechanism –of the structural system in equilibrium. This consideration makes it possible to utilize the residual tensile capacity up to 90% of the average strength [22,40]. This as-

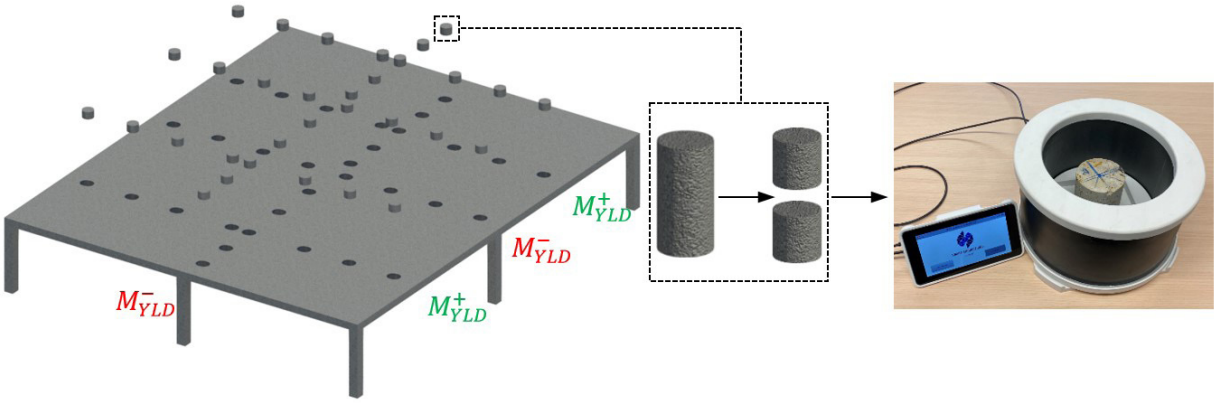

Figure 8. Cored flat slab and inductive testing for determining the amount, distribution and orientation of fibres.

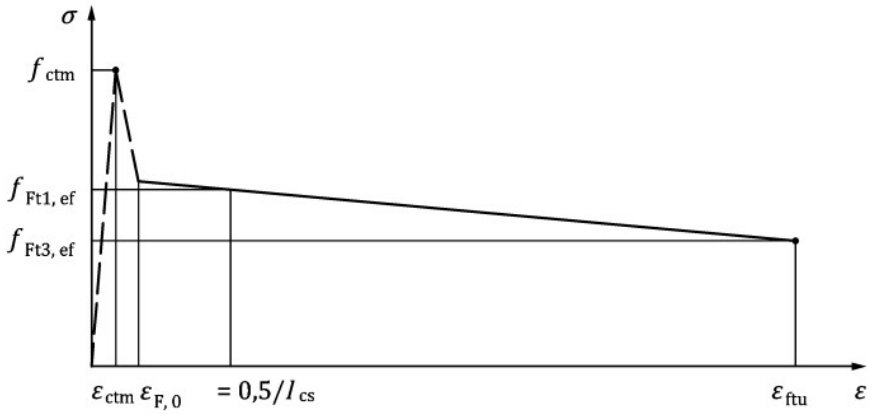

Figure 9. Tri-linear stress-strain constitutive law for simulating the mechanical response of SFRC subjected to uniaxial tension.

sumption is based on the fact that the scatter of the residual tensile strength of the SFRC decreases with the increase of the volume of material subjected to tension involved in the failure mechanism (i.e., length of the yield line). For local failure mechanisms –independently of the structural redundancy- and small cracked areas, a k_G = 1.0 shall be considered.

The relation $f_{R,1k}/f_{ctk,0.05} \geq 0.5$ must be satisfied to guarantee material ductility to avoid either a fragile response in case of lightly reinforced elements or any crack localization. Considering that the characteristic value of the residual tensile strength for SLS (f_{Ftsk}) is 0,40 $f_{R,1k}$ (assuming $k_o = k_G = 1.0$), the ratio $f_{R,1k}/f_{ctk,0.05} \geq 0.5$ results in $f_{Ftsk}/f_{ctk,0.05} \geq 0.2$ and, thus, that the residual tensile capacity of the SFRC must be equal or superior than 20% of $f_{ctk,0.05}$.

In local analyses, for critical cross-sections responsible for the structural equilibrium –of part or the entire structure-, the contribution of fibres has to be disregarded. Likewise, this applies to tying systems for robustness of building (L.12.5) and for connections and supports subjected to compression (L.13.2).

3.4. Stress-strain relation for structural analysis

For structural analysis by means of using numerical tools, a tri-linear constitutive law is proposed (see Figure 9 and Eq. 3-6) for simulating the uniaxial stress-strain of SFRC subjected to tension. The pre-cracking and crack initiation stage are assimilated to the response of a plain concrete (PC), and the residual response is simulated through a linear strain softening or hardening—depending on the SFRC strength class—until reaching the ultimate tensile uniaxial strain of the material (ε_{ftu}). This approach is similar to that proposed in the *fib* Model Code 2010 and the *fib* Bulletin 105 [32,40].

$$f_{Ft1,ef} = k_o \, k_G \, 0.37 \, f_{R,1k} \tag{3}$$

$$f_{Ft3,ef} = k_o \, k_G \, (0.57 \, f_{R,3k} - 0.26 \, f_{R,1k}) \tag{4}$$

$$\varepsilon_{F,0} = | \, 2 \, \varepsilon_{ctm} = f_{ctm} / E_{cm} \tag{5}$$

$$\varepsilon_{F,0} = \frac{w_u}{l_{cs}} \leq 2.5 \, \frac{mm}{l_{cs}} < \varepsilon_{Fud} = 0.02 \tag{6}$$

In Eq. 3 and 4, k_o is the fibre orientation factor and k_G is the factor accounting for the effect of member size. In Eq. 6, the structural characteristic length lcs is obtained as l_{cs}=min (h; $s_{r,m,cal,F}$) for members subjected to combined axial and bending and as $l_{cs} = s_{r,m,cal,F}$ for members subjected to uniaxial tension ($s_{r,m,cal,F}$ is the mean crack spacing, see Eq. 16). As it can be observed, l_{cs} can be considered as a double factor considering size effect and synergy of the fibres and rebars contributions. In structural elements with SFRC where cracking pattern is mainly governed by the rebars, lcs is computed as the cracks spacing. For low or not reinforced SFRC, lcs is evaluated as the element depth, as the equivalent hinge length.

When EN 14651 [15] specimens are considered l_{cs} = 125 mm as applied in Figure 9. The structural characteristic length lcs is considered jointly with the maximum crack opening (w_u) adopted for ULS to transform the localized crack opening in equivalent strain.

In the case of the stress-strain relation of SFRC subjected to short-term uniaxial compression, the same expression than for PC may be used, but by providing modifications in the compressive strain at mean compressive strength (ε_{c1}(‰) = $0.7f_{cm}^{1/3}$ (1+0.03$f_{R,1k}$)) and in the ultimate compressive strain (ε_{c1} = k ε_{c1}, where k = 1 + 20/√(82–2.2 $f_{R,1k}$)) [51–53].

3.5. *Properties of SFRC at high temperature*

The Annex B of the FprEN 1992-1-2:2023 [2] provides additional provisions to FprEN 1992-1-1:2023 Annex L [1] for the design of SFRC subjected to high temperatures. Only in this subsection, the Clauses cited are specifically referred to FprEN 1992-1-2:2023 [2].

Strength and deformation properties of SFRC in compression at elevated temperatures may be assumed as those for PC and computed according to the provisions provided in Clause 5. As per uniaxial tension SFRC properties at elevated temperatures, the stress-strain relationships proposed in the Annex L of FprEN 1992-1-1:2023 [1] can be considered; nonetheless, the strength parameters (f_{ctm}, $f_{Ft1,ef}$ and $f_{Ft3,ef}$) must be affected by a reduction coefficient $f_{ct,\theta}/f_{ctk,0.05}$ ($f_{ct,\theta}$ being the uniaxial tensile strength of concrete at temperature θ) to take into consideration the degradation of the mechanical properties caused by high elevated temperatures. In any case, if design methods given in Clauses 6 and 7 are used, any contribution of fibres shall be neglected.

A formulation to compute the reduction coefficient $f_{ct,\theta}/f_{ctk,0.05}$ is proposed in Clause 5, nevertheless, alternative formulations for deriving the constitutive law for SFRC subjected to uniaxial tensions at high temperatures may be considered provided the results are within the range of experimental evidence. To this end, the research and methods reported in [54–57] might be of reference for this purpose. Likewise, test procedures as those proposed in the RILEM Recommendation TC 129 MHT-part 4 [58] might also provide support to derive the pre- and post-cracking tensile properties of the SFRC subjected to high temperatures.

4. DURABILITY

The second generation of EC-2 brings a radically new concept of design for/verification of durability through the introduction of Exposure Resistance Classes (ERCs) based on performance [1,12,59], introduced for carbonation and chloride-induced corrosion (environmental exposure conditions XC, XD and XS). At the same time, an informative Annex P is offered to National Standardization Bodies (NSBs) that actually contains the approach for durability of the current EC-2 [60].

Nonetheless, whichever approach is adopted by an NSB, the concrete cover due to durability requirements, $c_{min,dur}$, in the case of SFRC applies only to the embedded reinforcement. In other words, for a given element type and environmental exposure conditions, $c_{min,dur}$ is unaffected by the presence of SFs. The only limitation placed on minimum cover in the case of SFRC is to avoid fibre accumulation. Therefore, a minimum cover of c_{min} = 20 mm to embedded reinforcement is prescribed for SFRC elements.

Hence, a conservative approach has been adopted – any potential benefit in terms of durability offered by SF inclusion has been neglected as $c_{min,dur}$ is determined in the same way as for an equivalent RC element [61]. At the same time, even though SFs close to the element surface may corrode and cause rust stains, spalling of concrete is unlikely to occur since generated tensile stresses caused by corrosion-derived products from SFs are low due to the small diameter of the fibres [12,62].

However, the fact that an outer "layer" of fibres might corrode in an SFRC element has caused the adoption of two design approaches which take this into account, differentiating between SFRC elements designed to be uncracked and cracked.

In the case of SFRC elements under environmental exposure conditions XC2–XC4, XD1–XD3, and XS1–XS3, designed to be uncracked at the serviceability limit state (SLS), when verifying those at the ultimate limit state (ULS), the tensile strength of SFRC at the greatest distance from the neutral axis shall be disregarded within a "sacrificial" layer of $c_{f,dur}$ = 10 mm from the exposed surface [1] (see Figure 10). It should be noted that this refers to the verification of ULS and the cracked state of the cross-section. The justification for such an approach for uncracked elements is found in recent studies that have shown a modification of bond between the fibres and the matrix in this outermost layer, in particular due to wet–dry exposures [63,64]. If this occurs, either a decrease/loss of bond may happen, or its increase, which may lead to fibre rupture.

In the case of SFRC elements under environmental exposure conditions XC2–XC4, XD1–XD3, and XS1–XS3, designed to be cracked at the serviceability limit state (SLS), when verifying those at ULS and SLS, the tensile strength of SFRC at the greatest distance from the neutral axis shall be disregarded within a "sacrificial" layer of $c_{f,dur}$ = k_{dur}·$c_{min,dur}$ from the exposed surface [1] (see Figure 10). The recommended value of kdur is 0.50, unless defined differently by a National Annex. This provision does not apply for stainless steel fibres nor during the construction phase. The provision rely on relatively recent literature [63–65].

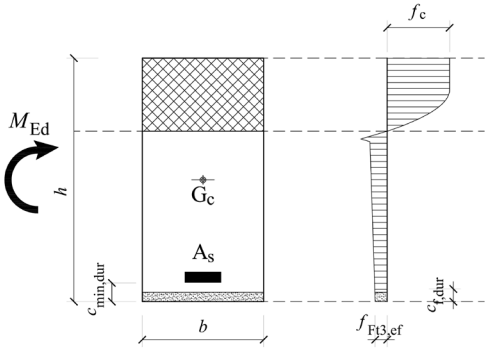

Figure 10. Definition of the "sacrificial" layer $c_{f,dur}$.

One of the main benefits of SFRC, i.e. reduced crack widths, may be taken into account for reducing the depth of the "sacrificial" layer $c_{f,dur}$:

$$c_{f,dur} = k_{dur}\ c_{min,dur}\ \frac{w_{k,cal}}{w_{lim,cal}} \geq 10\ mm \qquad (7)$$

where $w_{k,cal}$ and $w_{lim,cal}$ are the calculated and maximum permissible characteristic crack widths, i.e. the "sacrificial" layer depth can be reduced in proportion to the reduction of crack width relative to the limit.

It should be noted that the adopted approach disregards the potential corrosion of SFs on lateral surfaces of linear elements such as beams (i.e. no reduction of tensile strength is considered along the width of a section).

5. STRUCTURAL ANALYSIS – PLASTIC ANALYSIS

The combination of SFRC and longitudinal ordinary reinforcement –both with the suitable SC and quantity, respectively- has proven to provide sufficient rotation capacity of the bending-controlling cross-sections to allow for bending moment redistribution in statically indeterminate structures [14,27,30,32,66].

In this regard, the Annex L allows for a non-linear structural plastic analysis –or linear analysis with limited redistribution of forces– in ULS without a direct check of the capacity rotation in elements without ordinary reinforcement in (1) foundations and slabs supported directly on ground (even without ordinary reinforcement) and (2) for statically indeterminate rafts and pile-supported slabs. For the second group, a SFRC ductility class "c" is necessary and, if the member is needed for structural stability, a ratio $k_G \cdot f_{R,3k} / f_{ctm,fl} \geq 1.0$ (equivalent to bending-hardening response) is required. For this second group of elements, including elevated slabs, the rotation capacity is not necessary to be checked in (1) two-way systems with $L_x/L_y \leq 1.5$ and $A_s \geq A_{s,min}$, and (2) in both one- and two-way systems with $L_x/L_y > 1.5$ and $A_s \geq \alpha_{duct} \cdot A_{s,min}$. $A_{s,min}$ as per Clause L.12 (L_x/L_y). α_{duct} to be considered as 2.0 unless other recommended values are provided within National Annex.

For elements not fulfilling these sets of conditions, the compatibility between the ductility provided by the critical sections and that required for the plastic mechanism assumed (or redistribution level considered) must be checked accordingly. To this end, analyses as conducted in [67] [68] could be used to quantify the rotational capacity of critical SFRC cross-sections.

It must be remarked that, for members not fulfilling these conditions simultaneously, Annex L emphasizes that crack localization effects and, consequently, local reduction of the ductility could occur even if the minimum longitudinal reinforcement $A_{s,min}$ (according to L.12.1) is guaranteed. This aspect has been proved experimentally [69–75] and numerically [68] for statically both determinate and indeterminate beams.

Furthermore, the potential local variations of the residual tensile capacity of the SFRC should be considered appropriately as large cracked sections might present non-uniform ductility capacity.

6. ULTIMATE LIMIT STATES

6.1. Bending

The Annex L provides two simplified stress-strain constitutive models for simulating the residual tensile stress-strain response of SFRC members: a rigid-plastic behaviour and a bi-linear behaviour (see Figure 11).

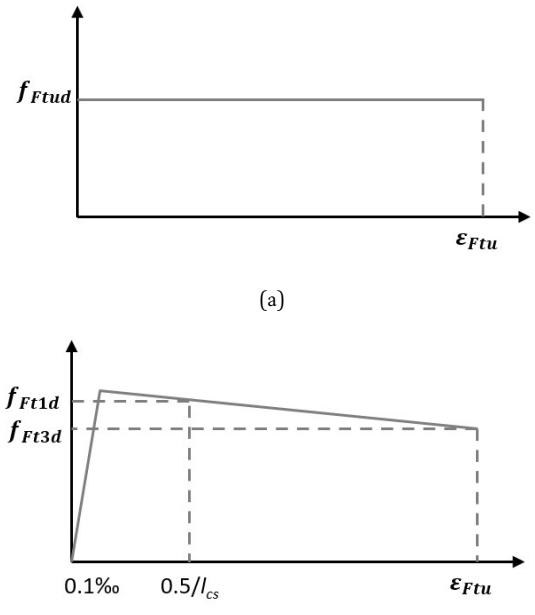

Figure 11. Simplified stress distributions for SFRC: (a) rigid-plastic distribution; (b) bi-linear distribution.

Referred to the bi-linear simplified stress distributions, the residual tensile strength and are defined according to:

$$f_{Ft1d} = f_{Ft1,ef} / \gamma_{SF} \qquad (8)$$

$$f_{Ft3d} = f_{Ft3,ef} / \gamma_{SF} \qquad (9)$$

The rigid-plastic approach proposed by the Annex L for flexural ULS design is consistent with the rigid-plastic constitutive model provided by the *fib* Model Code [40], which identifies the unique reference value f_{Ftud} as $f_{R3d}/3$ (Formula 5.6-4 in the *fib* Model Code [40]). This approach has proved to be reliable for evaluating the flexural strength of SFRC beams according to [76] and [71,77]. Based on the dataset of 53 SFRC beams assessed in [76], the mean of the model error (ratio of experimental-to-estimated flexural strength) for the *fib* Model Code [40] is 1.011 (coefficient of variation of the model of 8.0%). In addition, the trend of this error reduces with the increase of the SFRC residual flexural strength. Regarding RC beams with fibres, the *fib* Model Code predictions are also consistent according to the experimental program reported in [71,77] carried out on 42 standard beams with different types of fibres and longitudinal reinforcement ratios. Moreover, only for low longitudinal reinforcement ratios (around 0.5%) the addition of fibres significantly improves the flexural strength at ULS.

This rigid-plastic approach can be used for ductility classes a, b and c; for classes d and e, this approach should only be used to determine the ULS moment capacity at the design tensile strain limit ε_{Ftud}.

For sectional analysis at ULS (see Figure 12), fibre effect in SFRC is considered as a constant stress under the neutral axis corresponding to the residual tensile strength in uniaxial tension (according to the rigid-plastic model). In compression, parabola-rectangle or rectangular stress distribution proposed for PC can be assumed for SFRC by modifying the compressive strain at the peak stress (ε_{c2} = 0.0025) and the ultimate compressive strain (ε_{cu} = 0.006). These modifications of compressive strains are based on the studies carried out by Ruiz et al. [51–53] and de la Rosa et al. [78].

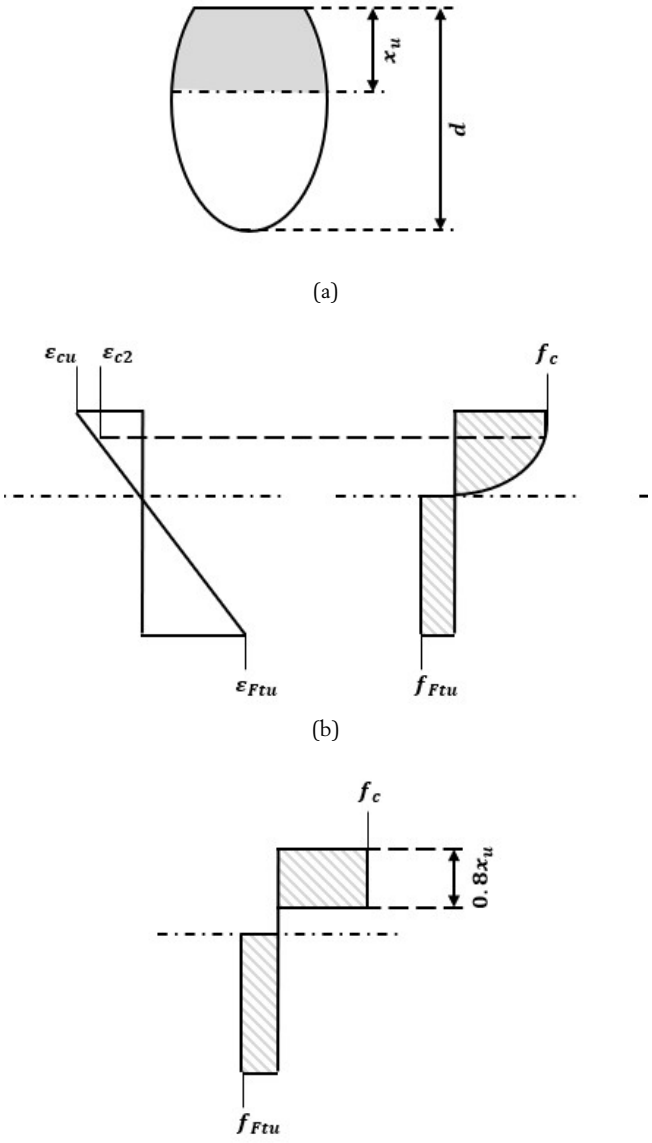

Figure 12. (a) Cross SFRC section; (b) strain distribution in SFRC section; (c) parabola-rectangle stress distribution in compression and constant stress in tension; (d) rectangular stress distribution in compression and constant stress distribution in tension.

6.2. Shear

The presence of steel fibres enhance the shear resistance of SFRC members since these are effective in controlling the opening of inclined cracks induced by shear stresses [79]. In fact, fibres allow a multiple and stable shear crack progression, delaying the formation of a single critical shear crack [80,81]. Hence, the addition of fibres improves the shear transfer across cracks, which results in an improvement of the aggregate interlock capacity [82] and, as a result, in an increase of the shear strength of SFRC members, as it is shown in Figure 13 [80,83–85] and Figure 14 [83,86].

In the Annex L, the shear strength formulation provided for RC members without shear reinforcement is modified to consider the fibre effect in SFRC members according to:

$$\tau_{Rd,cF} = \eta_{cF}\,\tau_{Rd,c} + \eta_F\,\tau_{Ftud} \geq \eta_{cF}\;\tau_{Rdc,min} + \eta_F f_{Ftud} \qquad (10)$$

where $\tau_{Rd,cF}$ is the design shear stress resistance of SFRC members without shear reinforcement, $\tau_{Rd,c}$ is the design shear stress resistance of RC members without shear reinforcement, is the design ultimate residual strength of ULS, $\tau_{Rdc,min}$ is the minimum design shear stress resistance allowing to avoid a detailed verification for shear, η_{cF} = max (1.2 – 0.5 f_{Ftuk};0.4) ≤ 1.0 and η_F=1.0.

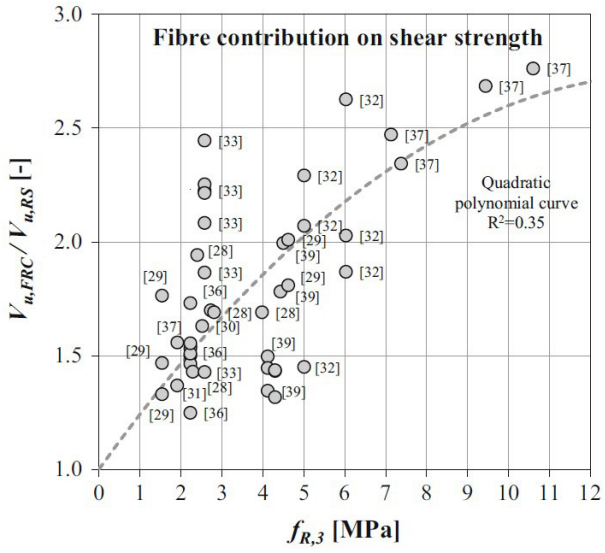

Figure 13. Increase in shear strength due to the effect of fibres in FRC members [87].

As it can be seen, the effect of fibres is described by an additional strength term f_{Ftud} and by introducing the parameter η to express that the fibre reinforcement term is not fully additive to the ordinary reinforced concrete contribution [12]. As for this, the shear strength of RC members is derived from the original formulation of the Critical Shear Crack Theory (CSCT) [88], whose failure criterion describes the shear resistance as a function of the reinforcement strain.

According to the CSCT, the shear resistance of members without stirrups is dependent on the critical shear crack width and on its roughness, since both parameters —influenced by the strain of the reinforcement, the size effect and the aggregate size— govern the aggregate interlock capacity. On this basis,

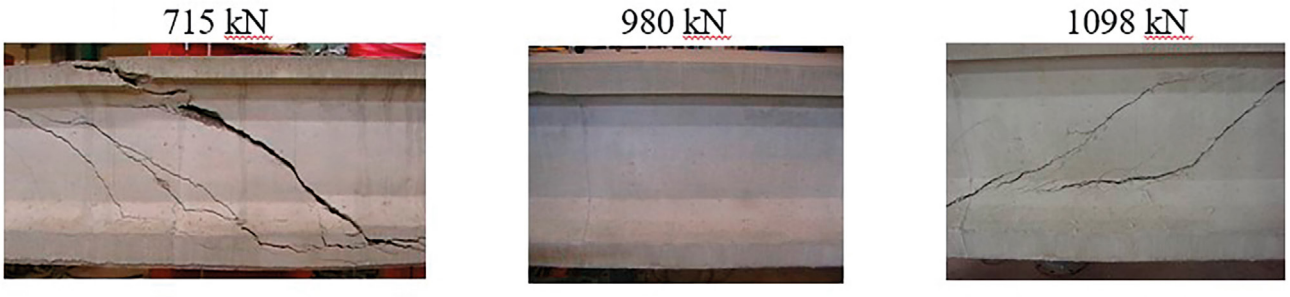

Figure 14. Shear crack patterns in prestressed beams with the same amount of transversal ordinary steel reinforcement for: (a) no fibres at 715 kN and SFRC for (b) 980 kN and (c) 1098 kN. [83,86].

close-form expressions for the calculation of the shear strength are proposed considering an improved general failure criterion —based on the refinement of the mechanical of the CSCT [89]— in combination with the load-deformation relationship. These new expressions have been validated considering a database with 669 shear tests resulting in good agreement when compared with test results and with no trends for the parameters investigated —shear span-to-effective depth ratio, longitudinal reinforcement, effective depth, width-to-effective depth ratio, compressive strength of the material, aggregate size [12].

Regarding the performance of SFRC members, a comprehensive shear database of 171 elements (93 in FRC and their 78 related in RC) was analysed in [87] to allow the development and validation of shear formulations. In this sense, it has been proved that the ratio shear span-to-effective depth ratio, the longitudinal reinforcement and the compressive strength of the material have similar influence on the shear strength both in RC and FRC members; however, it is different in the case of the size effect in shear. Related to this, the experimental results reported in [81] proved that fibres substantially mitigate the size effect in shear, showing that for effective depths above 1 m this effect is quite limited. Nevertheless, further studies are necessary to confirm this trend.

For SFRC members with shear reinforcement, Annex L also considers the fibre effect by an additional strength and by introducing the parameter f_{Ftud} to express that the fibre reinforcement and reinforced concrete contributions are not fully additive. The formulation provided results in:

$$\tau_{Rd,sF} = (\eta_{sw}\,\rho_w\,f_{ywd} + \eta_F\,f_{Ftud})\,cot\,\theta \geq \rho_w\,f_{ywd}\,cot\,\theta \qquad (11)$$

where $\tau_{Rd,sF}$ is the design shear stress resistance of SFRC members with shear reinforcement, ρ_w is the shear reinforcement ratio, f_{ywd} is the design yield strength of the shear reinforcement, f_{Ftud} is the design ultimate residual strength of ULS, θ is the angle of the compression field, $\eta_{sw} = 0.75$ and $\eta_F = 1.0$.

6.3. *Punching shear*

Several studies [90–93] have confirmed the effect of fibres for increasing the punching shear strength of SFRC slabs as well as their deformational capacity. This improvement is due to the bridging action of the fibres after the cracking of the concrete matrix [94]. Although this particular mechanical behaviour of SFRC slabs, code provisions have been adapted from the formulation of the RC elements [94]. Nevertheless, several specific models for punching shear of slab-column connections for elements with fibres have been proposed over the last decades [91,95–97]. In this regard, [94] gathers 140 test results from 13 different studies for assessing the punching shear strength of SFRC slab-column connections based on the CSCT [98,99]. It was confirmed that the concrete contribution to the punching strength decreases with the increase of the slab rotation, whereas the contribution of the fibres increases with it (see Figure 15).

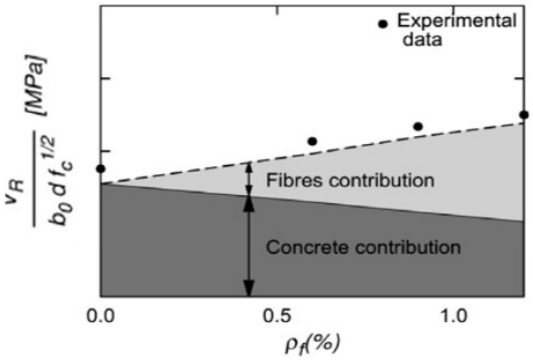

Figure 15. Fibres contribution to the punching shear strength for elements tested by Swamy and Ali [100] as reported in [94].

In a similar way that in the case of shear, the Annex L provides a punching shear formulation based on the CSCT considering an additional contribution to the punching shear stress resistance due to the presence of fibres. However, this contribution is not fully additive, as it is considered the parameter = 0.4. For SFRC without shear reinforcement, the punching shear resistance is obtained according to:

$$\tau_{Rd,cF} = \eta_c\,\tau_{Rd,c} + \eta_F\,f_{Ftud} \geq \eta_c\,\tau_{Rdc,min} + f_{Ftud} \qquad (12)$$

where $\tau_{Rd,cF}$ is the design punching shear stress resistance of SFRC members without shear reinforcement, $\tau_{Rd,c}$ is the design punching shear stress resistance of *RC* members without shear reinforcement, f_{Ftud} is the design ultimate residual strength of ULS, $\tau_{Rdc,min}$ is the minimum design punching shear stress resistance allowing to avoid a detailed verification for punching shear, $\eta_c \leq 1.0$ and $\eta_F = 0.4$.

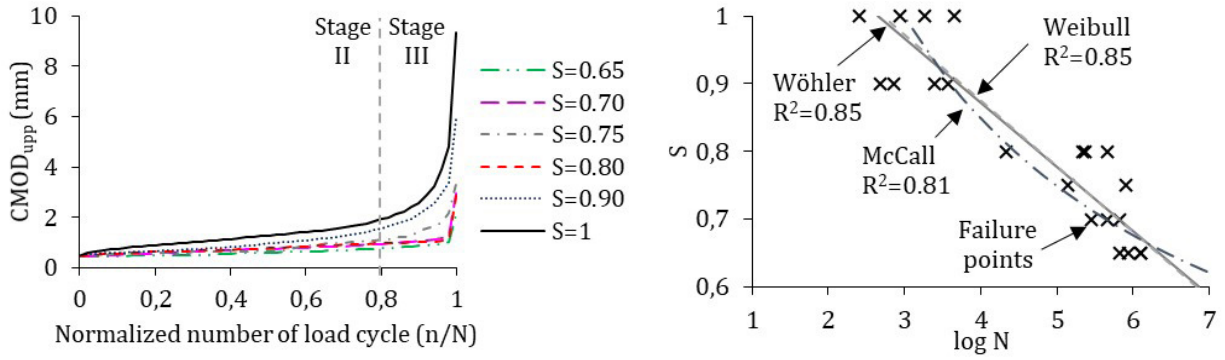

(a) (b)

Figure 16. (a) CMOD - n/N for different S and (b) different semi-probabilistic approaches for fitting the S - log N curves obtained experimentally.

In the case of elements with shear reinforcement, the contribution is also not fully additive and the punching shear resistance is obtained as follows:

$$\tau_{Rd,csF} = \eta_c \tau_{Rd,c} + \eta_s \rho_w f_{ywd} + \eta_F f_{Ftud} \geq \rho_w f_{ywd} + \eta_F f_{Ftud} \quad (13)$$

where $\tau_{Rd,csF}$ is the design punching shear stress resistance of SFRC members with shear reinforcement, $\tau_{Re,c}$ is the design punching shear stress resistance of RC members without shear reinforcement, ρ_w is the shear reinforcement ratio, f_{ywe} is the design yield strength of the shear reinforcement, f_{Ftud} is the design ultimate residual strength of ULS, $\eta_c \leq 1.0$, $\eta_{sw} = 0.75$ and $\eta_F = 0.4$.

6.4. Torsion

The provisions for torsion follow the philosophy adopted for shear: consideration of fibres as a smeared/distributed reinforcement and a reduction of the reinforced concrete (RC) contribution to torsion resistance as it is not considered fully additive with the fibre contribution:

$$\tau_{t,Rd,swF} = \eta_{sw} \tau_{t,Rd,swF} + \eta_F f_{Ftud} \geq \tau_{t,Rd,swF} \quad (14)$$

$$\tau_{t,Rd,slF} = \eta_{sw} \tau_{t,Rd,sl} + \eta_F f_{Ftud} \geq \tau_{t,Rd,sl} \quad (15)$$

where $\tau_{t,Rd,swF}$ and $\tau_{t,Rd,sw}$ are the torsional capacities of SFRC and RC, respectively, when governed by the yielding of the shear reinforcement; $\tau_{t,Rd,slF}$ and $\tau_{t,Rd,sl}$ are the torsional capacities of SFRC and RC, respectively, when governed by the yielding of the longitudinal reinforcement; f_{Ftud} is the design ultimate residual strength of SFRC; η_{sw} = 0.75 and η_F = 1.0. The torsional capacities $\tau_{t,Rd,sw}$ and $\tau_{t,Rd,sl}$ are calculated as for RC members according to the main text of EC-2 [1].

Additionally, when an SFRC member is subjected to a combination of torsion and shear and/or bending, two approaches are possible:

- considering that the fibre contribution is used to resist only torsional effects, or
- considering that the fibre contribution is used to resist only shear and/or bending effects (disregarding the fibre contribution to resisting torsional effects).

The provisions were tested on only a small number of available results [101], but a large safety margin was observed, justifying the approach [12].

6.5. Fatigue

Due to divergences found within the literature concerning the performance fatigue of FRC, the CEN/TC250/SC2 agreed on disregarding any potential contribution of steel fibres in compressive and/or tensile fatigue-induced stresses unless this contribution is proved by testing.

In this regard, there already exist SFRC structures designed to be subjected to fatigue-inducing loads, and allowed to crack in service conditions, as for instance: (1) rail-tracks embedded SFRC platforms [102,103], (2) floors and pavements [104] – the Spanish ROM 4.1-94 [105] allows the use of steel fibres as unique reinforcement of concrete pavements subjected to aggressive marine environments in combination with heavy static and dynamic loads–, (3) precast concrete towers for wind turbines [106], and others. Likewise, within the literature, there are several experimental programs and semi-probabilistic models on fatigue performance of cracked SFRC members subjected to direct tension [107,108], compression [109,110] and flexural [111–115] fatigue. Experimental constitutive crack mouth opening displacement (CMOD) - number of fatigue cycles (n) for pre-cracked SFRCs beams subjected to fatigue (Figure 16a) were provided in [114]. Likewise, several semi-probabilistic models (Figure 16b) that relate the load level (S) with the number of cycles to failure (N) were fitted based on experimental results.

As noted by the CEN/TC250/SC2, the scientific literature and current state-of-art on fatigue performance of SFRC allow confirming the marked stochastic nature -specially in pre-cracked elements subjected to direct tension or flexure- of the fatigue response of SFRC. Likewise, it is confirmed that there are numerous variables (i.e., pre-crack width, frequency and load range, amount and type of fibres, and others) which makes it difficult, at the current extent of knowledge, the derivation of general and robust conclusions and, thus, standardized provisions for fatigue of SFRC components.

7. SERVICEABILITY LIMIT STATES (SLS)

7.1. Crack control

One of the most well-known and proven benefits of using SFRC is crack control – the decrease of crack spacing and consequent decrease of crack widths. The new EC-2 presents an updated refined control of cracking relative to the current version, but the verification philosophy remains the same: a characteristic crack width is obtained by multiplying the calculated mean crack spacing $s_{r,m,cal}$ with the difference between the mean strain in the reinforcement and the mean strain in concrete ($\varepsilon s_m - \varepsilon_{cm}$) and multiplied by a factor k_w (1.7 if not specified otherwise by a National Annex) converting the mean crack width into a characteristic crack width (in fact the new EC-2 introduces one more factor $k_{1/r}$ that takes into account the increase in crack width due to curvature).

For SFRC, two cases are considered: (1) a multi-crack pattern associated to a presence of conventional reinforcement at a spacing ≤10Ø and (2) a single-crack pattern when the spacing of conventional reinforcement is larger than 10Ø. In the first case, the expression for $s_{r,m,cal}$ for RC is converted into $s_{r,m,cal,F}$ by multiplication of the second term of the original equation by $(1 - \alpha_f)$:

$$\tau_{r,m,cal,F} = 1.5\ c + \frac{k_{fl}\ k_b}{7.2}\ \frac{\phi}{\rho_{p,eff}}\ (1-\rho_f) \tag{16}$$

where c is the clear cover of the longitudinal reinforcement, k_{fl} is a factor accounting for the cross-section area in tension, k_b is a factor accounting for bond conditions, ϕ is the bar diameter, $\rho_{p,eff}$ is the reinforcement ratio of the effective tensile zone and $(1 - \rho_f)$ is an expression accounting for the crack arresting effect of SRFC as:

$$\alpha_f = \frac{f_{Ft1,ef}}{f_{ctm}} \leq 1.0 \tag{17}$$

In other words, the ratio of the effective residual strength associated to SLS (and a strain $0.5/l_{cs}$) to the axial tensile strength determines the crack spacing reduction, with a minimum value of $1.5c$ at $f_{Ft1,ef} = f_{ctm}$. The performance of the expression was validated on experimental results [116].

In the second case of elements with a single-crack pattern, the calculated mean crack spacing is given simply as:

$$s_{r,m,cal,F} = h - x \tag{18}$$

where x is the depth of the compression zone.

A final important point is that the conversion factor k_w is 1.7 and 1.3 for cases (1) and (2), i.e. multi-crack and single-crack patterns, respectively (though these values can be changed as the Annex L is informative and clause 9.2.3(2) of the main text declares k_w a nationally determined parameter with a recommended value of 1.7).

7.2. Deflection control

The Annex L does not explicitly deal with deflection control nor provide direct guidance or provision for indirect or direct deflection control of SFRC members. Considering that, except for lightly reinforced SFRC members subject to clause L.14, all SFRC members compliant with provisions of Annex L will be reinforced with at least the minimum longitudinal steel reinforcement, it is safe to assume that the general ς-method of interpolating curvatures (or deflections) [1] is applicable to SFRC members as well.

In particular, at the fibre and fibre–matrix level, no significant effect of steel fibre and fibre–matrix creep is observed at normal temperatures [117]. However, at the structural level, several phenomena should be considered. Firstly, the presence of steel fibres will affect the tension stiffening, i.e. the contribution of concrete in tension between two cracks (affecting the ς interpolation coefficient), and secondly, the moment of inertia of a "fully cracked" SFRC section will be larger than a corresponding RC one due to the presence of fibres.

Although there is still no direct integration of these aspects into the ς-method, some research exists showing the way forward. Namely, in [118] an extension of the so-called tension chord model (TCM) to SFRC to model the tension stiffening effect is proposed. This model allowed to define tension stiffening stresses for minimum and maximum crack spacing scenarios. Following this result, in [119] the TCM model for SFRC to calculating instantaneous deflections of members in bending was applied; however, not following the approach of the ς-method but the deflection calculation method originally proposed in [120].

Therefore, work remains in this regard, both at the experimental level as full-scale sustained load tests on SFRC are scarce [121–123], as well as with regards to models that need to be developed.

8. DETAILING OF MEMBERS AND PARTICULAR RULES

8.1. General rules for minimum reinforcement

The residual bending capacity in ULS of a SFRC cross-section subjected to bending (and a concomitant design axial force, N_{Ed}) shall be superior to its cracking bending capacity (Eq. 19) to guarantee a ductile response immediately after the cracking.

$$M_{R,min}\ (N_{Ed}) \geq M_{cr}\ (N_{Ed}) \tag{19}$$

For computing $M_{R,min}$, the effective residual tensile strength of the SFRC in ULS ($f_{Ftu,ef}$) can be considered. The reduced $A_{s,min}$ due to the contribution of the fibres that satisfies Eq. 19 shall be compliant with the criteria presented in subsection 8.2.

The similar approach shall be considered for cross-sections subjected to pure tensile axial force ($M_{Rd} = 0$) by computing $A_{s,min}$ through the application of Eq. 19. $N_{R,min}$ and N_{cr} are the pure tensile capacity of SFRC in ULS and against cracking, respectively.

$$N_{R,min} \geq N_{cr} \tag{20}$$

Similarly, the effective contribution of fibres can be considered in ULS for shear and torsion resistant mechanisms. The

a) b)

c) d)

Figure 17. SFRC segments subjected to loading transient situations inducing bending forces: (a) demoulding; (b) stacking; (c) manipulation and (d) final transport operation.

minimum shear reinforcement ratio ($\rho_{Fw,min}$) in SFRC elements requiring shear or torsion reinforcement can be computed by means of Eq. 21.

$$\rho_{Fw,min} = \rho_{w,min} - \frac{f_{Ftu,ef}}{f_{yk}} \geq 0 \quad (21)$$

where $\rho_{w,min}$ being the minimum transverse reinforcement, fyk the characteristic value of the steel (bars) yielding strength, and $f_{Ftu,ef} \geq 0.08 \cdot \sqrt{f_{ck}}$.

The minimum torsion reinforcement ratio ($\rho_{Fw,min}$) for SFRC requiring longitudinal and transverse reinforcement can be computed –for both types of reinforcements- according to Eq. 22.

$$\rho_{Fw,min} \geq \rho_{w,min} - \frac{f_{Ftu,ef}}{f_{yk}} \geq 0.3 \frac{f_{ctm}}{f_{yk}} \quad (22)$$

8.2. Particular rules for minimum reinforcement

For *beams*, the $A_{s,min}$ –minimum longitudinal reinforcement as per sectional ductility according to 9.2.2 of EC-2)– should be always guaranteed independently of the structural redundancy level of the beam. Contrarily, both the shear and torsion reinforcement can be totally replaced by the contribution of fibres if $f_{Ftu,ef}/f_{yk} \geq \rho_{Fw,min}$ and the other general rules presented in 8.1 are fulfilled.

In case of slabs, the Annex L allows for partial replacement of the longitudinal reinforcement, and for a reduction of $A_{s,min}$ so that $A_{s,min} \geq k_{AS}\, A_{s,min}$ (0.5 unless a country's National Annex establishes a different value). The secondary reinforcement in one-way slabs may be fully replaced by steel fibres. Regarding shear reinforcement, this may be fully replaced by steel fibres if the inequalities $f_{Ftu,ef}/f_{yk} \geq \rho_{Fw,min}$ and $f_{Ftu,ef} \geq 0.08 \cdot \sqrt{f_{ck}}$ are satisfied.

Finally, for walls and deep beams, both vertical ($As_{,min,v}$) and horizontal ($A_{s,min,h}$) minimum reinforcement computed according to Eq. 19 may be fully replaced.

9. LIGHTLY REINFORCED SFRC STRUCTURES

The Clause L.14 covers the design and detailing of structural SFRC elements reinforced with longitudinal reinforcement inferior to $A_{s,min}$. This clause may be only applied to statically indeterminate structures -some of those are identified in the Clause L.14.1.

As per understanding of the authors of this paper, other elements as those (1) designed no to crack –in either transient or permanent loading situations– and (2) that both the SFRC SC and ductility are sufficient to prevent the element from a fragile response in the unlikely event of cracking could also be covered by Clause L.14. This would be the case of, for example, precast SFRC segments for tunnel linings (Figure 17) since

these undergo transient loading situations (i.e., demoulding, staking, transport, manipulation) in which the segments are statically supported and subjected to bending [124–129].

It is remarked that ductility should be ensured -providing a suitable combination of fibres and longitudinal reinforcement- to avoid structural collapse in case of brittle failure in members constructed with crack-controlling joints. Likewise, it is emphasized that –independently of the minimum longitudinal reinforcement designed for both ductility and strength requirements– the reinforcement for SLS of cracking and for any local/global ULS must be designed accordingly.

For elements without longitudinal reinforcement, the residual shear strength of the SFRC in ULS ($\tau_{Rd,cF}$) may be taken as f_{Ftud}. Likewise, the Annex L remarks that lightly reinforced SFRC elements subjected to punching are not covered and have to be assessed by rigorous analyses.

Apart from other provisions within this Clause L.14, the Annex L specifies minimum SFRC strength and ductility classes for foundations directly on ground (1b), foundations on piles (2c) and tunnel lining segments without additional longitudinal reinforcement (4c). The latter specification is aligned with the recommendations gathered *fib* Bulletin 83 [130] and with outcomes reported in [131–133].

10. CONCLUSIONS

Since the DBV 2001 [4], the first national standard regulating the structural use of steel fibres, to the recently approved Spanish Structural Code 2020 [134], the Annex L of the new EC-2 represents a compendium of experience and knowledge related to the structural use (design, execution and quality control) of SFRC and a reference for the European countries.

The Annex L provides guide to design SFRC structures of any typology and of any structural responsibly (consequence failure class). Therefore, as SFRC has been introduced in the harmonized European guidelines for the first time, in order to adopt a prudent approach among the numerous member countries of CEN, the Annex L has the status of an Informative Annex and each CEN member has to decide its status within the country.

The scientific community is intensively researching on open topics to provide methods and tools that allow optimized design of SFRC components by considering the resistant mechanisms more accurately, as well as improved quality control procedures. A significant part of this research is promoted and boosted by the construction sector, which has seen interest in this material due to the identified (and proved) technical benefits as well as the enhanced sustainability performance respect to existing alternatives in a large variety of applications.

Notation

A_{ct} Tension area of the concrete cross section
A_s Cross-sectional area of ordinary reinforcement
$A_{s,min}$ Minimum ross-sectional area of reinforcement
M_{cr} Cracking moment of the section in presence of the simultaneous axial force N_{Ed}
$M_{R,min}$ Bending strength of the section with $A_{s,min}$ in presence of the simultaneous axial force N_{Ed}
N_{Ed} Design value of the applied axial force
Concrete cover
Minimum concrete cover c
Minimum concrete cover c due to durability requirement
d Effective depth of a cross section
Secant modulus of elasticity of concrete
Compressive strength of concrete
Characteristic concrete cylinder compressive strength
Mean concrete cylinder compressive strength
$f_{ctk,0.05}$ Characteristic axial tensile strength of concrete (5% fractile)
f_{ctm} Mean axial tensile strength of concrete
$f_{ctm,fl}$ Mean flexural tensile strength of concrete
$f_{ct,\theta}$ Tensile strength of concrete at temperature θ
$f_{Fts,ef}$ Effective value of the service residual strength (SFRC)
f_{Ftsd} Design value of the service residual strength (SFRC)
f_{Ftsk} Characteristic value of the service residual strength (SFRC)
$f_{Ftu,ef}$ Effective value of the ultimate residual strength (SFRC)
f_{Ftud} Design value of the ultimate residual strength (SFRC)
f_{Ftuk} Characteristic value of the ultimate residual strength (SFRC)
f_R Residual flexural strength (SFRC)
$f_{R,1d}$ Design value of the residual flexural strength for crack mouth opening displacements of 0.5 mm (SFRC)
$f_{R,1k}$ Characteristic value of the residual flexural strength for crack mouth opening displacements of 0.5 mm (SFRC)
$f_{R,3d}$ Design value of the residual flexural strength for crack mouth opening displacements of 2.5 mm (SFRC)
$f_{R,3k}$ Characteristic value of the residual flexural strength for crack mouth opening displacements of 2.5 mm (SFRC)
f_{Rk} Characteristic value of the residual flexural strength (SFRC)
f_{yk} Characteristic value of yield strength of reinforcement
f_{ywd} Design yield strength of shear reinforcement
h Overall depth of a cross section
k_G Factor accounting for the effect of member size (SFRC)
k_o Fibre orientation factor (SFRC)
l_{cs} Structural characteristic length
$s_{r,m,cal,F}$ Calculated mean crack spacing (SFRC)
$w_{k,cal}$ Calculated crack width
$w_{lim,cal}$ Limiting crack width to be compared with the calculated crack width $w_{k,cal}$
w_u Maximum crack opening at the ultimate limit state (SFRC)
x Depth of concrete in compression
x_u Depth of the neutral axil at the ultimate limit state after redistribution
γ_{SF} Partial factor for fibers in concrete
ε_{c1} Compressive strain in the concrete at mean compressive strength
ε_{c2} Compressive strain in the concrete at the peak stress f_c
ε_{cm} Mean strain in the concrete between cracks at the same level of ε_{sm}
ε_{ctm} Mean strain in the concrete at peak stress f_{ctm}
ε_{cu} Ultimate compressive strain in the concrete
$\varepsilon_{F,0}$ Strain in the concrete equal to $2\cdot \varepsilon_{ctm}$ (SFRC)
ε_{Ftu} Ultimate tensile strain in concrete (SFRC)
ε_{Ftud} Design value of the ultimate tensile strain in concrete (SFRC)
ε_{sm} Mean strain in the reinforcement closest to the most tensioned concrete surface under the relevant

combination of actions.

Θ Angle between the compression field and the member axis

$\rho_{p,eff}$ Tensile reinforcement ratio accounting for the different bond properties of reinforcing bars referred to the effective concrete area

ρ_{w} Shear reinforcement ratio

$\rho_{Fw,min}$ Minimum shear reinforcement ratio (SFRC)

$\rho_{w,min}$ Minimum shear reinforcement ratio

$\rho_{Rd,c}$ Design stress resistance of members without shear reinforcement

$\rho_{Rd,cF}$ Design stress resistance of members without shear reinforcement (SFRC)

$\rho_{Rd,csF}$ Design stress resistance of planar members with shear reinforcement (SFRC)

$\rho_{Rd,sF}$ Design stress resistance of members with shear reinforcement (SFRC)

$\rho_{Rdc,min}$ Minimum shear stress resistance allowing to avoid a detailed verification of shear (SFRC)

Ø Diameter of a reinforcing bar

References

[1] FprEN 1992-1-1:2023, Eurocode 2: Design of concrete structures – Part 1-1: General rules, rules for buildings, bridges and civil engineering structures, CEN, Brussels, 2023. This document is available through the National members at CEN TC250/SC Eurocode 2.

[2] FprEN 1992-1-2:2023, Eurocode 2: Design of concrete structures – Part 1-2: General rules - Structural fire design, CEN, Brussels, 2023. This document is available through the National members at CEN TC250/SC Eurocode 2.

[3] M. di Prisco, G. Plizzari, L. Vandewalle, Fibre reinforced concrete: new design perspectives, Mater. Struct. 42 (2009) 1261–1281. https://doi.org/10.1617/s11527-009-9529-4.

[4] DBV-Merkblatt, Stahlfaserbeton, 2001.

[5] RILEM TC162-TDF, Test and design methods for steel fibre reinforced concrete σ-ε design method, Mater. Struct. Constr. 36 (2003) 560–567. https://doi.org/10.1617/14007.

[6] CNR-DT 204/2006, Guide for the Design and Construction of Fiber-Reinforced Concrete Structures, Rome, 2007.

[7] EHE, Instrucción de Hormigón Estructural (EHE-08), 2008. https://doi.org/10.1017/CBO9781107415324.004.

[8] SS 812310, Fibre Concrete - Design of Fibre Concrete Structures, 2014.

[9] A. de la Fuente, A. Blanco, J. Armengou, A. Aguado, Sustainability based-approach to determine the concrete type and reinforcement configuration of TBM tunnels linings. Case study: Extension line to Barcelona Airport T1, Tunn. Undergr. Sp. Technol. 61 (2017) 179–188. https://doi.org/10.1016/j.tust.2016.10.008.

[10] A. de La Fuente, M.D.M. Casanovas-Rubio, O. Pons, J. Armengou, Sustainability of Column-Supported RC Slabs: Fiber Reinforcement as an Alternative, J. Constr. Eng. Manag. 145 (2019) 1–12. https://doi.org/10.1061/(ASCE)CO.1943-7862.0001667.

[11] I. Josa, A. de la Fuente, M.M. del M. Casanovas-Rubio, J. Armengou, A. Aguado, Sustainability-oriented model to decide on concrete pipeline reinforcement, Sustain. 13 (2021) 3026. https://doi.org/10.3390/su13063026.

[12] CEN/TC 250/SC 2/WG 1, Background Document for prEN 1992-1-1:2021, Brussels, 2021. This document is available through the National members at CEN TC250/SC Eurocode 2.

[13] EN 1990, Eurocode - Basis of structural design, CEN, Brussels, 2002.

[14] M. Di Prisco, M. Colombo, D. Dozio, Fibre-reinforced concrete in fib Model Code 2010: principles, models and test validation, Struct. Concr. 14 (2013) 342–361. https://doi.org/10.1002/SUCO.201300021.

[15] EN 14651, Test method for metallic fibred concrete — Measuring the flexural tensile strength (limit of proportionality (LOP), residual), Br. Stand. Inst. (2005). https://doi.org/9780580610523.

[16] G. Tiberti, F. Germano, A. Mudadu, G.A. Plizzari, An overview of the flexural post-cracking behavior of steel fiber reinforced concrete, Struct. Concr. 19 (2018) 695–718. https://doi.org/10.1002/suco.201700068.

[17] E. Galeote, Á. Picazo, M.G. Alberti, A. De La Fuente, A. Enfedaque, J. Gálvez, A. Aguado, Statistical analysis of an experimental database on residual flexural strengths of fiber reinforced concretes: Performance-based equations, Struct. Concr. (2022) 1–14.

[18] S.H.P. Cavalaro, A. Aguado, Intrinsic scatter of FRC: an alternative philosophy to estimate characteristic values, Mater. Struct. Constr. 48 (2015) 3537–3555. https://doi.org/10.1617/s11527-014-0420-6.

[19] P. Martinelli, M. Colombo, A. de la Fuente, S. Cavalaro, P. Pujadas, M. di Prisco, Characterization tests for predicting the mechanical performance of SFRC floors: design considerations, Mater. Struct. Constr. 54 (2021). https://doi.org/10.1617/s11527-020-01598-2.

[20] P. Martinelli, M. Colombo, P. Pujadas, A. de la Fuente, S. Cavalaro, M. di Prisco, Characterization tests for predicting the mechanical performance of SFRC floors: identification of fibre distribution and orientation effects, Mater. Struct. Constr. 54 (2021). https://doi.org/10.1617/s11527-020-01593-7.

[21] G. Žirgulis, O. Švec, E.V. Sarmiento, M.R. Geiker, A. Cwirzen, T. Kanstad, Importance of quantification of steel fibre orientation for residual flexural tensile strength in FRC, Mater. Struct. Constr. 49 (2016) 3861–3877. https://doi.org/10.1617/S11527-015-0759-3/METRICS.

[22] M. di Prisco, P. Martinelli, D. Dozio, The structural redistribution coefficient KRd: a numerical approach to its evaluation, Struct. Concr. 17 (2016) 390–407. https://doi.org/10.1002/SUCO.201500118.

[23] JCSS, Probabilistic Model Code, 2001.

[24] V. Cugat, S.H.P.P. Cavalaro, J.M. Bairán, A. de la Fuente, Safety format for the flexural design of tunnel fibre reinforced concrete precast segmental linings, Tunn. Undergr. Sp. Technol. 103 (2020) 103500. https://doi.org/10.1016/j.tust.2020.103500.

[25] J.M. Bairán, N. Tošić, A. De La Fuente, Reliability-based assessment of the partial factor for shear design of fibre reinforced concrete members without shear reinforcement, Mater. Struct. Constr. 54 (2021) 185. https://doi.org/10.1617/s11527-021-01773-z.

[26] V. Cervenka, Reliability-based non-linear analysis according to fib Model Code 2010, Struct. Concr. 14 (2013) 19–28. https://doi.org/10.1002/SUCO.201200022.

[27] L. Facconi, G. Plizzari, F. Minelli, Elevated slabs made of hybrid reinforced concrete: Proposal of a new design approach in flexure, Struct. Concr. 20 (2019) 52–67. https://doi.org/10.1002/SUCO.201700278.

[28] A. Nogales, A. de la Fuente, Numerical-aided flexural-based design of fibre reinforced concrete column-supported flat slabs, Eng. Struct. 232 (2021). https://doi.org/10.1016/j.engstruct.2020.111745.

[29] S. Aidarov, F. Mena, A. de la Fuente, Structural response of a fibre reinforced concrete pile-supported flat slab: full-scale test, Eng. Struct. 239 (2021). https://doi.org/10.1016/j.engstruct.2021.112292.

[30] S. Aidarov, N. Tošić, A. de la Fuente, A limit state design approach for hybrid reinforced concrete column-supported flat slabs, Struct. Concr. 23 (2022) 3444–3464. https://doi.org/10.1002/SUCO.202100785.

[31] EN 14889-1, Fibres for concrete - Part 1: Steel fibres, Brussels, 2006.

[32] fib Bulletin 105, Fibre Reinforced Concrete, Lausanne, 2023.

[33] E. García-Taengua, S. Arango, J.R. Martí-Vargas, P. Serna, Flexural creep of steel fiber reinforced concrete in the cracked state, Constr. Build. Mater. 65 (2014) 321–329. https://doi.org/10.1016/j.conbuildmat.2014.04.139.

[34] A. Llano-Torre, P. Serna Ros, S.H. Pialarissi Cavalaro, International round robin test on creep behavior of FRC supported by the RILEM TC 261-CCF, FRC Mod. Landscape. BEFIB 2016. Proc. 9th RILEM Int. Symp. Fibre Reinf. Concr. (2016) 127–140. https://upcommons.upc.edu/handle/2117/94235 (accessed February 18, 2023).

[35] A. Llano-Torre, P. Serna, S.H.P. Cavalaro, International Round-Robin Test on Creep Behaviour of FRC - Part 2: An Overview of Results and Preliminary Conclusions, RILEM Bookseries. 36 (2022) 291–306. https://doi.org/10.1007/978-3-030-83719-8_26/COVER.

[36] G. Plizzari, P. Serna, Structural effects of FRC creep, Mater. Struct. Constr. 51 (2018) 1–11. https://doi.org/10.1617/s11527-018-1290-0.

[37] P. Serna, S. Arango, T. Ribeiro, A.M. Núñez, E. Garcia-Taengua, Structural cast-in-place SFRC: Technology, control criteria and recent applications in spain, Mater. Struct. Constr. 42 (2009) 1233–1246. https://doi.org/10.1617/S11527-009-9540-9/METRICS.

[38] E.S. Bernard, G.G. Xu, Estimation of Population Standard Deviation for Post-Crack Performance of Fiber-Reinforced Concrete, Adv. Civ. Eng. Mater. 6 (2017) 68–82.

[39] E.S. Bernard, G.G. Xu, Normality of post-crack performance data for fiber-reinforced concrete, Adv. Civ. Eng. Eng. Mater. 8 (2019) 145–157.

[40] FIB, fib Model Code for Concrete Structures 2010, International Federation for Structural Concrete (fib), Lausanne, 2013. https://doi.org/10.1002/9783433604090.

[41] M. Di Prisco, L. Ferrara, M.G.L. Lamperti, Double edge wedge splitting (DEWS): An indirect tension test to identify post-cracking behaviour of fibre reinforced cementitious composites, Mater. Struct. Constr. 46 (2013) 1893–1918. https://doi.org/10.1617/S11527-013-0028-2/METRICS.

[42] C. Molins, A. Aguado, S. Saludes, Double punch test to control the energy dissipation in tension of FRC (Barcelona test), Mater. Struct. Constr. 42 (2009) 415–425. https://doi.org/10.1617/s11527-008-9391-9.

[43] P. Pujadas, A. Blanco, S.H.P.P. Cavalaro, A. De La Fuente, A. Aguado, Multidirectional double punch test to assess the post-cracking behaviour and fibre orientation of FRC, Constr. Build. Mater. 58 (2014) 214–224. https://doi.org/10.1016/j.conbuildmat.2014.02.023.

[44] P. Pujadas, A. Blanco, S. Cavalaro, A. De La Fuente, A. Aguado, New Analytical Model To Generalize the Barcelona Test Using Axial Displacement, J. Civ. Eng. Manag. 19 (2013) 259–271. https://doi.org/10.3846/13923730.2012.756425.

[45] E. Galeote, A. Blanco, S.H.P.P. Cavalaro, A. de la Fuente, Correlation between the Barcelona test and the bending test in fibre reinforced concrete, Constr. Build. Mater. 152 (2017) 529–538. https://doi.org/10.1016/j.conbuildmat.2017.07.028.

[46] EN 206, Concrete - Specification, performance, production and conformity, CEN, Brussels, 2013.

[47] J.M. Torrents, A. Blanco, P. Pujadas, A. Aguado, P. Juan-García, M.Á. Sánchez-Moragues, Inductive method for assessing the amount and orientation of steel fibers in concrete, Mater. Struct. Constr. 45 (2012) 1577–1592. https://doi.org/10.1617/s11527-012-9858-6.

[48] A. Blanco, P. Pujadas, A. De La Fuente, S.H.P. Cavalaro, A. Aguado, Assessment of the fibre orientation factor in SFRC slabs, Compos. Part B Eng. 68 (2015) 343–354. https://doi.org/10.1016/j.compositesb.2014.09.001.

[49] S.H.P. Cavalaro, R. López, J.M. Torrents, A. Aguado, Improved assessment of fibre content and orientation with inductive method in SFRC, Mater. Struct. Constr. 48 (2015) 1859–1873. https://doi.org/10.1617/s11527-014-0279-6.

[50] S.H.P. Cavalaro, R. López-Carreño, J.M. Torrents, A. Aguado, P. Juan-García, Assessment of fibre content and 3D profile in cylindrical SFRC specimens, Mater. Struct. Constr. 49 (2016) 577–595. https://doi.org/10.1617/s11527-014-0521-2.

[51] P.G. Ruiz, M.F., Muttoni, A. and Gambarova, Relationship between nonlinear creep and cracking of concrete under uniaxial compression, J. Adv. Concr. Technol. 5 (2007) 383–393.

[52] G. Ruiz, A. de la Rosa, E. Poveda, R. Zanon, M. Schäfer, S. Wolf. Compressive behaviour of steel-fibre reinforced concrete in Annex L of new Eurocode 2, Hormigón y Acero (2022). https://doi.org/10.33586/hya.2022.3092

[53] G. Ruiz, Á. de la Rosa, S. Wolf, E. Poveda, Model for the compressive stress–strain relationship of steel fiber-reinforced concrete for non-linear structural analysis, Hormigón y Acero. 69 (2018) 75–80. https://doi.org/10.1016/J.HYA.2018.10.001.

[54] M. Colombo, M. Di Prisco, R. Felicetti, SFRC exposed to high temperature: Hot vs. residual characterization for thin walled elements, Cem. Concr. Compos. 58 (2015) 81–94. https://doi.org/10.1016/J.CEMCONCOMP.2015.01.002.

[55] F. Di Carlo, A. Meda, Z. Rinaldi, Evaluation of the bearing capacity of fiber reinforced concrete sections under fire exposure, Mater. Struct. Constr. 51 (2018) 1–12. https://doi.org/10.1617/S11527-018-1280-2/FIGURES/13.

[56] R. Serafini, R.R. Agra, R.P. Salvador, A. De La Fuente, A.D. De Figueiredo, Double Edge Wedge Splitting Test to Characterize the Design Postcracking Parameters of Fiber-Reinforced Concrete Subjected to High Temperatures, J. Mater. Civ. Eng. 33 (2021). https://doi.org/10.1061/(ASCE)MT.1943-5533.0003701.

[57] R. Serafini, R.R. Agra, J. Bitencourt L.A.G., A. de la Fuente, A.D. de Figueiredo, Bond-slip response of steel fibers after exposure to elevated temperatures: Experimental program and design-oriented constitutive equation, Compos. Struct. 255 (2021). https://doi.org/10.1016/j.compstruct.2020.112916.

[58] R.T. 129-M.T. methods for mechanical properties of concrete at High, temperatures, Part 4: Tensile strength for service and accident conditions, Mater. Struct. 33 (2000) 219–223.

[59] C. Andrade, D. Izquierdo, Durability and Cover Depth Provisions in Next Eurocode 2. Background Modelling and Calculations and Cover Depth Provisions, Hormigón y Acero. (2023). https://doi.org/https://doi.org/10.33586/hya.2023.3102.

[60] EN 1992-1-1, Eurocode 2: Design of concrete structures - Part 1-1: General rules and rules for buildings, CEN, Brussels, 2004.

[61] S.C. Paul, G.P.A.G. van Zijl, B. Šavija, Effect of fibers on durability of concrete: A practical review, Materials (Basel). 13 (2020) 1–26. https://doi.org/10.3390/ma13204562.

[62] P.S. Mangat, K. Gurusamy, Chloride diffusion in steel fibre reinforced marine concrete, Cem. Concr. Res. 17 (1987) 385–396. https://doi.org/10.1016/0008-8846(87)90002-0.

[63] V. Marcos-Meson, Durability of steel fibre reinforced concrete in corrosive environments, Technical University of Denmark, 2019.

[64] P. Hagelia, Deterioration Mechanisms and Durability of Sprayed Concrete for Rock Support in Tunnels, Technical University of Delft, 2011.

[65] V. Marcos-Meson, A. Michel, A. Solgaard, G. Fischer, C. Edvardsen, T.L. Skovhus, Corrosion resistance of steel fibre reinforced concrete - A literature review, Cem. Concr. Res. 103 (2018) 1–20. https://doi.org/10.1016/J.CEMCONRES.2017.05.016.

[66] H. Salehian, J.A.O. Barros, Assessment of the performance of steel fibre reinforced self-compacting concrete in elevated slabs, Cem. Concr. Compos. 55 (2015) 268–280. https://doi.org/10.1016/J.CEMCONCOMP.2014.09.016.

[67] P. Schumacher, Rotation capacity of self-compacting steel fibre reinforced concrete, TU Delft, 2006.

[68] A. Nogales, N. Toši, | Albert De La Fuente, N. Tošić, A. de la Fuente, Rotation and moment redistribution capacity of fiber- reinforced concrete beams : Parametric analysis and code compliance, Struct. Concr. (2021) 1–20. https://doi.org/10.1002/suco.202100350.

[69] H.C. Mertol, E. Baran, H.J. Bello, Flexural behavior of lightly and heavily reinforced steel fiber concrete beams, Constr. Build. Mater. 98 (2015) 185–193. https://doi.org/10.1016/J.CONBUILDMAT.2015.08.032.

[70] A.N. Dancygier, E. Berkover, Cracking localization and reduced ductility in fiber-reinforced concrete beams with low reinforcement ratios, Eng. Struct. 111 (2016) 411–424. https://doi.org/10.1016/J.ENGSTRUCT.2015.11.046.

[71] A. Conforti, R. Zerbino, G. Plizzari, Assessing the influence of fibers on the flexural behavior of reinforced concrete beams with different longitudinal reinforcement ratios, Struct. Concr. 22 (2021) 347–360. https://doi.org/10.1002/SUCO.201900575.

[72] P. Visintin, M.S. Mohamad Ali, T. Xie, A.B. Sturm, Experimental investigation of moment redistribution in ultra-high performance fibre reinforced concrete beams, Constr. Build. Mater. 166 (2018) 433–444. https://doi.org/10.1016/J.CONBUILDMAT.2018.01.156.

[73] D.Y. Yoo, D.Y. Moon, Effect of steel fibers on the flexural behavior of RC beams with very low reinforcement ratios, Constr. Build. Mater. 188 (2018) 237–254. https://doi.org/10.1016/J.CONBUILDMAT.2018.08.099.

[74] T. Markić, A. Amin, W. Kaufmann, T. Pfyl, Strength and Deformation Capacity of Tension and Flexural RC Members Containing Steel Fibers, J. Struct. Eng. 146 (2020) 04020069. https://doi.org/10.1061/(ASCE)ST.1943-541X.0002614.

[75] T. Markić, A. Amin, W. Kaufmann, T. Pfyl, Discussion on "Assessing the influence of fibers on the flexural behavior of reinforced concrete beams with different longitudinal reinforcement ratios" by Conforti et al. [structural concrete, 2020], Struct. Concr. 22 (2021) 1888–1891. https://doi.org/10.1002/suco.202000488.

[76] S.J. Foster, A. Parvez, Assessment of model error for reinforced concrete beams with steel fibers in bending, Struct. Concr. 20 (2019) 1010–1021. https://doi.org/10.1002/SUCO.201800090.

[77] A. Conforti, R. Zerbino, G. Plizzari, Influence of steel, glass and polymer fibers on the cracking behavior of reinforced concrete beams under flexure, Struct. Concr. 1 (2018) 133–143.

[78] Á. de la Rosa, G. Ruiz, E. Poveda, Study of the Compression Behavior of Steel-Fiber Reinforced Concrete by Means of the Response Surface

Methodology, Appl. Sci. 2019, Vol. 9, Page 5330. 9 (2019) 5330. https://doi.org/10.3390/APP9245330.

[79] W. Kaufmann, A. Amin, A. Beck, M. Lee, Shear transfer across cracks in steel fibre reinforced concrete, Eng. Struct. 186 (2019) 508–524. https://doi.org/10.1016/J.ENGSTRUCT.2019.02.027.

[80] F. Minelli, G.A. Plizzari, On the effectiveness of steel fibers as shear reinforcement, ACI Struct. J. 110 (2013) 2013. https://doi.org/10.14359/51685596.

[81] F. Minelli, A. Conforti, E. Cuenca, G. Plizzari, Are steel fibres able to mitigate or eliminate size effect in shear?, Mater. Struct. Constr. 47 (2014) 459–473. https://doi.org/10.1617/S11527-013-0072-Y/METRICS.

[82] J. Navarro-Gregori, E.J. Mezquida-Alcaraz, P. Serna-Ros, J. Echegaray-Oviedo, Experimental study on the steel-fibre contribution to concrete shear behaviour, Constr. Build. Mater. 112 (2016) 100–111. https://doi.org/10.1016/J.CONBUILDMAT.2016.02.157.

[83] E. Cuenca, On shear behavior of structural elements made of steel fiber reinforced concrete, Universitat Politècnica de València, 2015.

[84] A. Amin, S.J. Foster, Shear strength of steel fibre reinforced concrete beams with stirrups, Eng. Struct. 111 (2016) 323–332. https://doi.org/10.1016/J.ENGSTRUCT.2015.12.026.

[85] J.A.O. Barros, S.J. Foster, An integrated approach for predicting the shear capacity of fibre reinforced concrete beams, Eng. Struct. 174 (2018) 346–357. https://doi.org/10.1016/J.ENGSTRUCT.2018.07.071.

[86] E. Cuenca, P. Serna, Failure modes and shear design of prestressed hollow core slabs made of fiber-reinforced concrete, Compos. Part B Eng. 45 (2013) 952–964. https://doi.org/10.1016/J.COMPOSITESB.2012.06.005.

[87] E. Cuenca, A. Conforti, F. Minelli, G.A. Plizzari, J. Navarro Gregori, P. Serna, A material-performance-based database for FRC and RC elements under shear loading, Mater. Struct. Constr. 51 (2018) 11. https://doi.org/10.1617/s11527-017-1130-7.

[88] A. Muttoni, M.F. Ruiz, Shear strength of members without transverse reinforcement as function of critical shear crack width, ACI Struct. J. 105 (2008) 163–172. https://doi.org/10.14359/19731.

[89] FIB Bulletin 85, Towards a rational understanding of shear in beams and slabs, Lausanne, 2018.

[90] S.D.B. Alexander, S.H. Simmonds, Punching Shear Tests of Concrete Slab-Column Joints Containing Fiber Reinforcement, Struct. J. 89 (1992) 425–432. https://doi.org/10.14359/3027.

[91] M.H. Harajli, D. Maalouf, H. Khatib, Effect of fibers on the punching shear strength of slab-column connections, Cem. Concr. Compos. 17 (1995) 161–170. https://doi.org/10.1016/0958-9465(94)00031-S.

[92] P.J. McHarg, W.D. Cook, D. Mitchell, Y.S. Yoon, Benefits of concentrated slab reinforcement and steel fibers on performance of slab-column connections, ACI Struct. J. 97 (2000) 225–234. https://doi.org/10.2/JQUERY.MIN.JS.

[93] M.Y. Cheng, G.J. Parra-Montesinos, Evaluation of Steel Fiber Reinforcement for Punching Shear Resistance in Slab-Column Connections— Part I: Monotonically Increased Load, ACI Struct. J. 107 (2010) 101–109.

[94] L.F. Maya, M. Fernández Ruiz, A. Muttoni, S.J. Foster, Punching shear strength of steel fibre reinforced concrete slabs, Eng. Struct. 40 (2012) 83–94. https://doi.org/10.1016/J.ENGSTRUCT.2012.02.009.

[95] R. Narayanan, I.Y.S. Darwish, Punching shear tests on steel-fibre-reinforced micro-concrete slabs, Https://Doi.Org/10.1680/Macr.1987.39.138.42. 39 (2015) 42–50. https://doi.org/10.1680/MACR.1987.39.138.42.

[96] K.K. Choi, M.M. Reda Taha, H.G. Park, A.K. Maji, Punching shear strength of interior concrete slab–column connections reinforced with steel fibers, Cem. Concr. Compos. 29 (2007) 409–420. https://doi.org/10.1016/J.CEMCONCOMP.2006.12.003.

[97] H. Higashiyama, A. Ota, M. Mizukoshi, Design Equation for Punching Shear Capacity of SFRC Slabs, Int. J. Concr. Struct. Mater. 5 (2011) 35–42. https://doi.org/10.4334/IJCSM.2011.5.1.035.

[98] A. Muttoni, Punching shear strength of reinforced concrete slabs without transverse reinforcement, ACI Struct. J. 105 (2008) 440–450. https://doi.org/10.14359/19858.

[99] J.T. Simões, M. Fernández Ruiz, A. Muttoni, Validation of the Critical Shear Crack Theory for punching of slabs without transverse reinforcement by means of a refined mechanical model, Struct. Concr. 19 (2018) 191–216. https://doi.org/10.1002/SUCO.201700280.

[100] R.N. Swanmy, S.A.R. Ali, Punching Shear Behavior of Reinforced Slab-Column Connections Made with Steel Fiber Concrete, J. Proc. 79 (1982) 392–406. https://doi.org/10.14359/10917.

[101] V.V. Oettel, Torsionstragverhalten von stahlfaserbewehrten Beton-, Stahlbeton und Spannbetonbalken, TU Braunschweig, 2016.

[102] M. Tarifa, X.X. Zhang, G. Ruiz, E. Poveda, Full-scale fatigue tests of precast reinforced concrete slabs for railway tracks, Eng. Struct. 100 (2015) 610–621. https://doi.org/10.1016/J.ENGSTRUCT.2015.06.016.

[103] M. Domingo, G. Ramos, Á.C. Aparicio, Use of fiber reinforced concrete in bridges – Metrorrey Line 2 case study, Eng. Struct. 276 (2023) 115373. https://doi.org/10.1016/J.ENGSTRUCT.2022.115373.

[104] B. Belletti, R. Cerioni, A. Meda, G. Plizzari, Design Aspects on Steel Fiber-Reinforced Concrete Pavements, J. Mater. Civ. Eng. 20 (2008) 599–607. https://doi.org/10.1061/(ASCE)0899-1561(2008)20:9(599).

[105] Puertos del estado, ROM 4.1-94: Guidelines for the design and construction of port pavements, 1994.

[106] The Concrete Center, Concrete Towers for Onshore and Offshore Wind Farms, 2007.

[107] G.A. Plizzari, S. Cangiano, S. Alleruzzo, The Fatigue Behaviour of Cracked Concrete, Fatigue Fract. Eng. Mater. Struct. 20 (1997) 1195–1206. https://doi.org/10.1111/J.1460-2695.1997.TB00323.X.

[108] J. Zhang, H. Stang, V.C. Li, Experimental Study on Crack Bridging in FRC under Uniaxial Fatigue Tension, J. Mater. Civ. Eng. 12 (2000) 66–73. https://doi.org/10.1061/(ASCE)0899-1561(2000)12:1(66).

[109] L. Saucedo, R.C. Yu, A. Medeiros, X. Zhang, G. Ruiz, A probabilistic fatigue model based on the initial distribution to consider frequency effect in plain and fiber reinforced concrete, Int. J. Fatigue. 48 (2013) 308–318. https://doi.org/10.1016/J.IJFATIGUE.2012.11.013.

[110] A. Medeiros, X. Zhang, G. Ruiz, R.C. Yu, M.D.S.L. Velasco, Effect of the loading frequency on the compressive fatigue behavior of plain and fiber reinforced concrete, Int. J. Fatigue. 70 (2015) 342–350. https://doi.org/10.1016/J.IJFATIGUE.2014.08.005.

[111] J.-L. Granju, P. Rossi, P. Rivillon, G. Chanvillard, B. Mesureur, A. Turatsinze, Delayed behaviour of cracked SFRC beams, Fifth Int. RILEM Symp. Fibre-Reinforced Concr. (2000) 511–520.

[112] F. Germano, G. Tiberti, G. Plizzari, Post-peak fatigue performance of steel fiber reinforced concrete under flexure, Mater. Struct. Constr. 49 (2016) 4229–4245. https://doi.org/10.1617/S11527-015-0783-3/METRICS.

[113] S.J. Stephen, R. Gettu, Fatigue fracture of fibre reinforced concrete in flexure, Mater. Struct. Constr. 53 (2020) 1–11. https://doi.org/10.1617/S11527-020-01488-7/METRICS.

[114] D.M. Carlesso, S. Cavalaro, A. de la Fuente, Flexural fatigue of pre-cracked plastic fibre reinforced concrete: Experimental study and numerical modeling, Cem. Concr. Compos. 115 (2021). https://doi.org/10.1016/j.cemconcomp.2020.103850.

[115] H. Fataar, R. Combrinck, W.P. Boshoff, An Experimental Study on the Flexural Fatigue Behaviour of Pre-cracked Steel Fibre Reinforced Concrete, RILEM Bookseries. 36 (2022) 155–165. https://doi.org/10.1007/978-3-030-83719-8_14/COVER.

[116] G. Tiberti, F. Minelli, G. Plizzari, Cracking behavior in reinforced concrete members with steel fibers: A comprehensive experimental study, Cem. Concr. Res. 68 (2015) 24–34. https://doi.org/10.1016/J.CEMCONRES.2014.10.011.

[117] N. Tošić, S. Aidarov, A. de la Fuente, Systematic Review on the Creep of Fiber-Reinforced Concrete, Materials (Basel). 13 (2020) 5098.

[118] A. Amin, S.J. Foster, M. Watts, Modelling the tension stiffening effect in SFR-RC, Mag. Concr. Res. 68 (2016) 339–352. https://doi.org/10.1680/macr.15.00188.

[119] A. Amin, S.J. Foster, W. Kaufmann, Instantaneous deflection calculation for steel fibre reinforced concrete one way members, Eng. Struct. 131 (2017) 438–445. https://doi.org/10.1016/j.engstruct.2016.10.041.

[120] A. Kenel, P. Nellen, A. Frank, P. Marti, Reinforcing steel strains measured by Bragg grating sensors, J. Mater. Civ. Eng. 17 (2005) 423–431. https://doi.org/10.1061/(ASCE)0899-1561(2005)17:4(423).

[121] K.H. Tan, P. Paramasivam, K.C. Tan, Instantaneous and long-term deflections of steel fiber reinforced concrete beams, ACI Struct. J. 91 (1994) 384–393.

[122] K.H. Tan, P. Paramasivam, K.C. Tan, Creep and shrinkage deflections of RC beams with steel fibers, J. Mater. Civ. Eng. 6 (1994) 474–494.

[123] E. Vasanelli, F. Micelli, M.A. Aiello, G. Plizzari, Long term behavior of FRC flexural beams under sustained load, Eng. Struct. 56 (2013) 1858–1867. https://doi.org/10.1016/j.engstruct.2013.07.035.

[124] G.A. Plizzari, G. Tiberti, Steel fibers as reinforcement for precast tunnel segments, Tunn. Undergr. Sp. Technol. 21 (2006) 438–439. https://doi.org/10.1016/j.tust.2005.12.079.

[125] B. Chiaia, A.P. Fantilli, P. Vallini, Evaluation of minimum reinforcement ratio in FRC members and application to tunnel linings, Mater. Struct. Constr. 40 (2007) 593–604. https://doi.org/10.1617/s11527-006-9166-0.

[126] B. Chiaia, A.P. Fantilli, P. Vallini, Combining fiber-reinforced concrete with traditional reinforcement in tunnel linings, Eng. Struct. 31 (2009) 1600–1606. https://doi.org/10.1016/j.engstruct.2009.02.037.

[127] A. Caratelli, A. Meda, Z. Rinaldi, P. Romualdi, Structural behaviour of precast tunnel segments in fiber reinforced concrete, Tunn. Undergr. Sp. Technol. 26 (2011) 284–291. https://doi.org/10.1016/j.tust.2010.10.003.

[128] A. Caratelli, A. Meda, Z. Rinaldi, Design according to MC2010 of a fibre-reinforced concrete tunnel in Monte Lirio, Panama, Struct. Concr. 13 (2012) 166–173. https://doi.org/10.1002/SUCO.201100034.

[129] A. la Fuente, P. Pujadas, A. Blanco, A. Aguado, A. De la Fuente, P. Pujadas, A. Blanco, A. Aguado, Experiences in Barcelona with the use of fibres in segmental linings, Tunn. Undergr. Sp. Technol. 27 (2012) 60–71. https://doi.org/10.1016/j.tust.2011.07.001.

[130] FIB Bulletin 83, Precast Tunnel Segments in Fibre-Reinforced Concrete, International Federation for Structural Concrete (fib), Lausanne, 2018.

[131] F. Di Carlo, A. Meda, Z. Rinaldi, Design procedure for precast fibre-reinforced concrete segments in tunnel lining construction, Struct. Concr. 17 (2016) 747–759. https://doi.org/10.1002/SUCO.201500194.

[132] L. Liao, A. de la Fuente, S. Cavalaro, A. Aguado, Design of FRC tunnel segments considering the ductility requirements of the Model Code 2010, Tunn. Undergr. Sp. Technol. 47 (2015) 200–210. https://doi.org/10.1016/j.tust.2015.01.006.

[133] L. Liao, A. de la Fuente, S. Cavalaro, A. Aguado, Design procedure and experimental study on fibre reinforced concrete segmental rings for vertical shafts, Mater. Des. 92 (2016) 590–601. https://doi.org/10.1016/j.matdes.2015.12.061.

[134] Código Estructural, 2020.